2nd INTERNATIONAL WORKSHOP NSFDE&A'22

SOZOPOL, BULGARIA

NUMERICAL SOLUTION OF FRACTIONAL DIFFERENTIAL EQUATIONS AND APPLICATIONS

S. HARIZANOV, R. LAZAROV, I. LIRKOV, S. MARGENOV (EDS.)

INTERNATIONAL WORKSHOP

NSFDE&A'22

SOZOPOL, BULGARIA

NUMERICAL SOLUTION OF FRACTIONAL DIFFERENTIAL EQUATIONS AND APPLICATIONS

PROCEEDINGS OF SHORT COMMUNICATIONS

S. HARIZANOV, R. LARAROV, I. Lirkov, S. MARGENOV (EDS.)

Editors

Stanislav Harizanov
Bulgarian Academy of Sciences
Sofia, Bulgaria

Raytcho Lazarov
Texas A&M University
College Station, Texas, US

Ivan Lirkov
Bulgarian Academy of Sciences
Sofia, Bulgaria

Svetozar Margenov
Bulgarian Academy of Sciences
Sofia, Bulgaria

ISBN 978-619-7320-10-7 (eBook)

Institute of Information and Communication Technologies, Bulgarian Academy of Sciences,
Acad. G. Bonchev Str., Bl. 25A, 1113 Sofia, Bulgaria, 2020

PREFACE

The International Workshop on Numerical Solution of Fractional Differential Equations and Applications (NSFDE&A'22) is organized by the Institute of Information and Communication Technologies, Bulgarian Academy of Sciences, in cooperation with the Bulgarian Section of SIAM and the Center of Excellence in Informatics and Information and Communication Technologies (CoE in Informatics and ICT).

The CoE in Informatics and ICT, Grant No BG05M2OP001-1.001-0003, is financed by the Science and Education for Smart Growth Operational Program (2014-2020) and co-financed by the EU through the European Structural and Investment Funds.

The workshop follows the great success of the first workshop NSFDE&A'20 (http://parallel.bas.bg/Conferences/NSFDE&A_2020-Sozopol.pdf), and the Special Sessions "Fractional Diffusion Problems: Numerical Methods, Algorithms and Applications" organized within the scientific program of the 12th and 13th LSSC Conferences (http://parallel.bas.bg/Conferences/SciCom21/). The workshop is aimed to continue the new chain of NSFDE&A events to be organized biannually, every even year, complementary to the well-established LSSC conferences every odd year.

The major specific topics of NSFDE&A'22 include: (i) fractional in space diffusion problems; (ii) fractional in time diffusion problems; (iii) models of phenomena with memory; (iv) optimal control involving fractional diffusion; (v) analytical and semi-analytical solution methods; (vi) multigrid solvers; (vii) coupled problems; (viii) phase separation and image segmentation; (ix) parallel algorithms and HPC and big data tools; (x) applications in science and engineering.

List of keynote speakers and lectures:

- Lidia Aceto (University of Eastern Piedmont, Alessandria, Italy)
  Numerical approximations of fractional powers of operators
- Natalia Kopteva (University of Limerick, Ireland)
  Pointwise-in-time a-priori and a-posteriori error control for time-fractional parabolic equations
- Vaughan Voller (University of Minnesota, Minneapolis, USA)
  Enthalpy solution of a two-dimensional fractional Stefan problem

The purpose of the workshop is to bring together scientists in the field of numerical methods working with fractional differential equations models in natural sciences and environmental and industrial applications, as well as developers of algorithms for modern high-performance computers. The keynote lectures review some of the most advanced achievements in the field of numerical solution of fractional differential equations and their applications. The workshop talks are presented by scientists from diverse research institutions including applied mathematicians, numerical analysts, and computer experts.

Scientists from all over the world (America, Asia, and Europe) contributed to the success of the workshop, representing some of the strongest research groups in the field of the event.

This volume contains 29 short communications by authors from 12 countries.

The next International Workshop on NSFDE&A will be organized in June 2024.

Stanislav Harizanov
Raytcho Lazarov
Ivan Lirkov
Svetozar Margenov

Contents

Numerical approximations of fractional powers of operators

Lidia Aceto
Università del Piemonte Orientale
viale Teresa Michel, 11
15121 - Alessandria, Italy

In this talk we present numerical approximations of $\mathcal{L}^{-\alpha}, \alpha \in (0,1)$. Here $\mathcal{L}$ is a self-adjoint positive operator acting in an Hilbert space $\mathcal{H}$ in which the eigenfunctions of $\mathcal{L}$ form an orthonormal basis of $\mathcal{H}$, so that $\mathcal{L}^{-\alpha}$ can be written through the spectral decomposition of $\mathcal{L}$. In other words, for a given $g \in \mathcal{H}$, we have

$$\mathcal{L}^{-\alpha} g = \sum_{j=1}^{+\infty} \mu_j^{-\alpha} \langle g, \varphi_j \rangle \varphi_j \tag{1}$$

where μ_j and φ_j are the eigenvalues and the eigenfunctions of $\mathcal{L}$, respectively, and $\langle \cdot, \cdot \rangle$ denotes the $\mathcal{H}$-inner product.

Applications of (1) include the numerical solution of fractional equations involving the anomalous diffusion, in which $\mathcal{L}$ is related to the standard Laplace operator.

In recent years, this problem has been studied by many authors. In the continuous setting of unbounded operators, methods based on the best uniform rational approximation (BURA) of functions closely related to $\lambda^{-\alpha}$ have been considered, for example, in [8, 9, 10, 11] by using a modified version of the Remez algorithm. Another class of methods relies on quadrature rules for the integral representation of $\lambda^{-\alpha}$ [1, 3, 4, 5, 6, 7, 12, 13].

Starting from the integral representation given in [6, Eq. (4)]

$$\mathcal{L}^{-\alpha} = \frac{2\sin(\alpha\pi)}{\pi} \int_0^{+\infty} t^{2\alpha-1} (\mathcal{I} + t^2 \mathcal{L})^{-1} dt, \qquad \alpha \in (0,1), \tag{2}$$

where $\mathcal{I}$ is the identity operator in $\mathcal{H}$, after appropriate changes of variables we consider approximations based on truncated quadrature rules. We present practical error estimates that can be used to select *a-priori* the number of quadrature points necessary to obtain a given accuracy. Some numerical experiments are also shown to demonstrate the reliability of the proposed approach.

References

[1] Aceto, L., Bertaccini, D., Durastante, F. and Novati, P. 2019 *Rational Krylov methods for functions of matrices with applications to fractional partial differential equations*. J. Comput. Phys. 396, 470–482.

[2] Aceto, L. and Novati, P. 2022 *Exponentially convergent trapezoidal rules to approximate fractional powers of operators*. J. Sci. Comput., in press.

[3] Aceto, L. and Novati, P. 2021 *Fast and accurate approximations to fractional powers of operators*. IMA Journal of Numerical Analysis. drab002, https://doi.org/10.1093/imanum/drab002

[4] Aceto, L. and Novati, P. 2020 *Padé-type approximations to the resolvent of fractional powers of operators*. J. Sci. Comput. 83, 13.

[5] Aceto, L. and Novati, P. 2019 *Rational approximations to fractional powers of self-adjoint positive operators*. Numer. Math. 143, 1–16.

[6] Bonito, A. and Pasciak, J.E. 2015 *Numerical approximation of fractional powers of elliptic operators*. Math. Comp. 84, 2083–2110.

[7] Bonito, A. and Pasciak, J.E. 2019 *On sinc quadrature approximations of fractional powers of regularly accretive operators*. J. Numer. Math. 27, 57–68.

[8] Harizanov, S., Lazarov, R., Margenov, S., Marinov, P. and Vutov, Y. 2018 *Optimal solvers for linear systems with fractional powers of sparse SPD matrices*. Numer. Linear Algebra Appl. 25, no. 5, e2167.

[9] Harizanov, S., Lazarov, R., Marinov, P., Margenov, S. and Pasciak, J.E. 2020 *Analysis of numerical methods for spectral fractional elliptic equations based on the best uniform rational approximation*. J. Comput. Phys. 408, 109285.

[10] Harizanov, S., Lazarov, R., Marinov, P., Margenov, S. and Pasciak, J.E. 2019 Comparison analysis of two numerical methods for fractional diffusion problems based on the best rational approximations of t^γ on $[0, 1]$. In *Advanced Finite Element Methods with Applications. FEM 2017* (ed. T. Apel, U. Langer, A. Meyer and O. Steinbach). Lecture Notes in Computational Science and Engineering, vol. 128. Springer.

[11] Harizanov, S. and Margenov, S. 2018 Positive approximations of the inverse of fractional powers of SPD M-Matrices. In *Control Systems and Mathematical Methods in Economics* (ed. G. Feichtinger, R. Kovacevic and G. Tragler). Lecture Notes in Economics and Mathematical Systems, vol. 687. Springer.

[12] Vabishchevich, P.N. 2020 *Approximation of a fractional power of an elliptic operator*. Linear Algebra Appl. 27, e2287.

[13] Vabishchevich, P.N. 2018 *Numerical solution of time-dependent problems with fractional power elliptic operator*. Comput. Meth. in Appl. Math. 18, no. 1, 111–128.

Second order approximations of the Caputo derivative with variable parameters

Stoyan Apostolov[1], Yuri Dimitrov[2,3],Venelin Todorov[3,4]
[1]Faculty of Mathematics and Informatics, Sofia University
[2] Department of Mathematics, Physics and Informatics,
University of Forestry
[3]Institute of Mathematics and Informatics,
Bulgarian Academy of Sciences
[4]Institute of Information and Communication Technologies,
Bulgarian Academy of Sciences

The present paper is a continuation of the work in [1,2]. We construct second order approximations of the Caputo derivative whose parameters have variable values, which depend on the number n of the nodes of a uniform mesh on the interval of fractional differentiation $[x_0,x]$. Let $h=(x-x_0)/n$. The L1 approximation of the Caputo derivative has an asymptotic formula [3]

$$\mathscr{L}_n[y]=\frac{1}{\Gamma(2-\alpha)h^\alpha}\sum_{k=0}^{n-1}\sigma_k^{(\alpha)}y_{n-k}=y_n^{(\alpha)}+\frac{\zeta(\alpha-1)}{\Gamma(2-\alpha)}y_n''h^{2-\alpha}+O\left(h^2\right), \tag{1}$$

$$\sigma_0^{(\alpha)}=1,\quad \sigma_k^{(\alpha)}=(k-1)^{1-\alpha}-2k^{1-\alpha}+(k+1)^{1-\alpha},\quad \sigma_n^{(\alpha)}=(n-1)^{1-\alpha}-n^{1-\alpha}.$$

In [4] we construct second order shifted approximations of the first derivative. In [1,2] we apply the method from [4] for construction of approximations of the second derivative. We derive the approximation of the second derivative

$$\mathscr{C}_n^B[y]=\frac{1}{h^2}\sum_{k=0}^{m}w_k(B)y_{m-k}=y_m''+\gamma_1(B)y_m'''h+\gamma_2(B)y_m^{(4)}h^2+\gamma_3(B)y_m^{(5)}h^3+O\left(h^4B^4\right), \tag{2}$$

where the function y satisfies the condition $y(x_0)=y'(x_0)=0$ and

$$w_0(B)=\frac{2}{B^2}\left(B-\ln(1+B)\right),\ w_1(B)=-\frac{2}{1+B},\ w_k(B)=\frac{2}{B^2k}\left(\frac{B}{1+B}\right)^k,\quad (k\geq 2),$$

$$\begin{aligned}\gamma_1(B) &= -\frac{1}{3}(2B+3),\\ \gamma_2(B) &= \frac{1}{12}(6B^2+12B+7),\\ \gamma_3(B) &= -\frac{1}{60}(2B^3+60B^2+50B+15).\end{aligned}$$

By substituting the second derivative in (1) with approximation (2) we find

$$\overline{\mathscr{L}}_n[y] = \frac{1}{\Gamma(2-\alpha)h^\alpha}\sum_{k=0}^{n-1}\delta_k^{(\alpha)}y_{n-k} = y_n^{(\alpha)} + O\left(h^2\right), \tag{3}$$

where $\delta_k^{(\alpha)} = \sigma_k^{(\alpha)} - \zeta(\alpha-1)w_k(B)$. When B is a fixed number approximation (2) of the Caputo derivative has a second order accuracy [1,2].

1 Approximation of the second derivative

In this section we construct an approximation of the second derivative as a weighted average of approximations (2) which have parameters $B, 2B, 3B$. Let c_1, c_2, c_3 be the solutions of the following system of equations

$$\begin{aligned} c_1 + \quad & c_2 + \quad & c_3 = 1\\ \gamma_1(B)c_1 + \gamma_1(2B)c_2 + \gamma_1(3B)c_3 &= 0\\ \gamma_2(B)c_1 + \gamma_2(2B)c_2 + \gamma_2(3B)c_3 &= 0.\end{aligned}$$

Consider the approximation $\mathscr{D}_n^B = c_1\mathscr{C}_n^B + c_2\mathscr{C}_n^{2B} + c_3\mathscr{C}_n^{3B}$ of the second derivative.

$$\mathscr{D}_n^B[y] = \frac{1}{h^2}\sum_{k=0}^{n} W_k y_{n-k} = y_n'' + \gamma y_n^{(5)}h^3 + O\left(h^4B^4\right), \tag{4}$$

$$\gamma = c_1\gamma_3(B) + c_2\gamma_3(2B) + c_3\gamma_3(3B) = -\frac{1}{60}(12B^3+33B^2+22B+50),$$
$$W_k = c_1w_k(B) + c_2w_k(2B) + c_3w_k(3B), \qquad (0 \le k \le n).$$

Approximation (4) has weights

$$\begin{aligned}W_0 = \frac{1}{108B^4}\big(&6B(66B^2+54B+11) - 18(3B+1)(12B+11)\ln(1+B)\\ &+9(18B^2+36B+11)\ln(1+2B) - 2(12B^2+27B+11)\ln(1+3B)\big),\end{aligned}$$

$$W_1 = \frac{2(33B^2+45B+13)}{3(B+1)(2B+1)(3B+1)},$$

$$W_k = \frac{B^{k-4}}{k}\left(\frac{(3B+1)(12B+11)}{6(B+1)^k} - \frac{(18B^2+36B+11)2^k}{12(2B+1)^k} + \frac{(12B^2+27B+11)3^k}{54(3B+1)^k}\right).$$

Table 1: Error and order of approximations $\mathscr{C}_n^B$ and $\mathscr{D}_n^B$ for the function $\sin x$.

$h=\frac{1}{n}$	$\mathscr{C}_n$, $B=\sqrt{n}$		$\mathscr{D}_n$, $B=\sqrt{n}$		$\mathscr{D}_n$, $B=\sqrt[3]{n}$	
	Error	Order	Error	Order	Error	Order
0.000625	0.00961535	0.5238	2.2485×10^{-5}	1.4101	5.6194×10^{-7}	2.2473
0.0003125	0.00660463	0.5418	8.2392×10^{-6}	1.4484	1.3563×10^{-7}	2.0507
0.00015625	0.00465389	0.5050	2.8687×10^{-6}	1.5221	3.4836×10^{-8}	1.9610

When $y(x_0)=y'(x_0)=0$ and B is a large number, approximations (2) and (4) have accuracy $O(Bh)$ and $O(B^3h^3)$ respectively. When $B=\lfloor\sqrt{n}\rfloor$ approximations (2) and (4) have orders $1/2$ and $3/4$. When $B=\lfloor\sqrt[3]{n}\rfloor$ the orders of (2) and (4) are $2/3$ and 2 respectively. The experimental results for the error and the order of approximations (2) and (4) for the function $y=\sin x$ are given in Table 1.

2 Second order approximation of the Caputo derivative

By approximating the second derivative in the expansion formula (1) of the L1 approximation with (4) we obtain the approximation of the Caputo derivative

$$\widetilde{\mathscr{L}_m}[y]=\frac{1}{\Gamma(2-\alpha)h^\alpha}\sum_{k=0}^{m-1}\lambda_k^{(\alpha)}y_{m-k}=y_m^{(\alpha)}+O\left(h^2\right), \tag{5}$$

where $\lambda_k^{(\alpha)}=\sigma_k^{(\alpha)}-\zeta(\alpha-1)W_k$. Approximation (5) has a second order when $y(x_0)=y'(x_0)=y''(x_0)=0$. Approximation (5) holds for all functions in $C^3[x_0,x_m]$ when

$$\widetilde{\mathscr{L}_m}[1]=0,\quad \widetilde{\mathscr{L}_m}[x]=\frac{1}{\Gamma(2-\alpha)}x^{1-\alpha},\quad \widetilde{\mathscr{L}_m}[x^2]=\frac{2}{\Gamma(3-\alpha)}x^{2-\alpha}, \tag{6}$$

Let

$$s_1=-\sum_{k=0}^{m-1}\lambda_k^{(\alpha)},\qquad s_2=\sum_{k=0}^{m-1}k\lambda_k^{(\alpha)},\qquad s_3=-\sum_{k=0}^{m-1}k^2\lambda_k^{(\alpha)},$$

$$S_1=s_1,\quad S_2=m^{1-\alpha}+ms_1+s_2,\quad S_3=\frac{2m^{2-\alpha}}{2-\alpha}+m^2s_1+2ms_2+s_3.$$

The numbers s_i and S_i are computed with $O(n)$ operations. By solving (6) with respect to the last three weights $\lambda_{m-2}^{(\alpha)},\lambda_{m-1}^{(\alpha)}$ and $\lambda_m^{(\alpha)}$ of approximation (5) we find

$$\lambda_{m-2}^{(\alpha)}=\frac{1}{2}\left(S_3-S_2\right),\quad \lambda_{m-1}^{(\alpha)}=2S_2-S_3,\quad \lambda_m^{(\alpha)}=\frac{1}{2}\left(2S_1-3S_2+S_3\right).$$

Example The two term ordinary fractional differential equation

$$y^{(\alpha)}(t)+Ly(t)=F(t),\qquad y(0)=y_0 \tag{7}$$

Table 2: Error and order of numerical solution (8) and $B = \lfloor \sqrt{n} \rfloor$.

$h = \frac{1}{n}$	$\alpha = 0.25$, $L = 1$		$\alpha = 0.5$, $L = 2$		$\alpha = 0.75$, $L = 3$	
	Error	Order	Error	Order	Error	Order
0.000625	9.5230×10^{-8}	1.9613	2.4524×10^{-7}	1.9662	4.6078×10^{-7}	1.9837
0.0003125	2.4370×10^{-8}	1.9662	6.2365×10^{-8}	1.9754	1.1598×10^{-7}	1.9901
0.00015625	6.2170×10^{-9}	1.9708	1.5784×10^{-8}	1.9822	2.9116×10^{-8}	1.9940

has a numerical solution [1,2]

$$u_m = \frac{1}{\lambda_0^{(\alpha)} + L\Gamma(2-\alpha)h^\alpha} \left(h^\alpha \Gamma(2-\alpha) F_n - \sum_{k=1}^{m} \lambda_k^{(\alpha)} u_{m-k} \right), \qquad (3 \leq m \leq n). \quad (8)$$

Numerical solution (8) has initial conditions $u_0 = y_0$ and

$$u_1 = \frac{y_0 + h^\alpha \Gamma(2-\alpha) F(h)}{1 + Lh^\alpha \Gamma(2-\alpha)}, \qquad u_2 = \frac{y_0 + (2h)^\alpha \Gamma(2-\alpha) F(2h)}{1 + L(2h)^\alpha \Gamma(2-\alpha)}.$$

The values of u_1 and u_2 are computed from the approximations (1)

$$y^{(\alpha)}(h) = \frac{y(h) - y(0)}{\Gamma(2-\alpha)h^\alpha} + O(h^{2-\alpha}), \qquad y^{(\alpha)}(2h) = \frac{y(2h) - y(0)}{\Gamma(2-\alpha)h^\alpha} + O(h^{2-\alpha}).$$

When $F(t) = x^\alpha E_{1,2-\alpha}(x) + Le^x$ equation (7) has a solution $y(t) = e^x$. The experimental results for the error and order of numerical solution (8) of equation (7) with $B = \lfloor \sqrt{n} \rfloor$ are given in Table 2.

3 Conclusions

In this paper we construct second order approximations of the Caputo derivative whose parameters have variable values. In future work we will apply the approximations for construction of finite difference schemes for numerical solution of ordinary and partial differential equations and and we will analyze the convergence of the numerical methods. We will also use the approximations for performing sensitivity analysis of complex models for smart information service networks [5].

Acknowledgements

This research has been partially supported by the Bulgarian National Science Fund under Project KP-06-M52/2 "Perspective Methods for Quality Prediction in the Next Generation Smart Information Service Networks" and by Project KP-06-N32/2 "Advanced Stochastic and Deterministic Approaches for Large-Scale Problems of Computational Mathematics".

References

[1] Apostolov S., Dimitrov Y., Todorov V., Constructions of second order approximations of the Caputo fractional derivative. In: Lirkov I., Margenov S. (eds) Large-Scale Scientific Computing. LSSC 2021. Lecture Notes in Computer Science, vol 13127. Springer (2022)

[2] Dimitrov, Y., Approximations for the second derivative and the Caputo fractional derivative, Proceedings of NSFDE&A'20, Sozopol, Bulgaria, pp. 16–18 (2020)

[3] Dimitrov, Y., A second order approximation for the Caputo fractional derivative, Journal of Fractional Calculus and Applications 7(2), (2016) 175–195

[4] Todorov V., Dimitrov Y., Dimov I., Second Order Shifted Approximations for the First Derivative. In: Dimov I., Fidanova S. (eds) Advances in High Performance Computing. HPC 2019. Studies in Computational Intelligence, vol 902. Springer, Cham (2021)

[5] Andonov, V., Poryazov, S., Saranova, E., Generalized Net Model of Overall Telecommunication System with Queueing. Advances and New Developments in Fuzzy Logic and Technology, 1308, Springer Verlag, 2021, ISBN:978-3-030-77715-9, 254-279

Numerical approximation and Bayesian inference of fractional SPDEs

David Bolin
Computer, Electrical and Mathematical Science
and Engineering Division,
King Abdullah University of Science and Technology,
Saudi Arabia

Some of the most popular models for Gaussian random fields in statistics and machine learning can be formulated as solutions to fractional stochastic partial equations (SPDEs). In this talk, we show how one can obtain accurate numerical approximations of such models by a combination of finite elements and rational approximations of the covariance operator of the Gaussian field.

The proposed method has been implemented in an R package with an interface to the popular R-INLA software for computationally efficient inference of latent Gaussian models. As an illustration of the power of the method, we present an inverse problem application in environmental statistics, where the parameters of a fractional SPDE, observed under Gamma distributed observations, are estimated. The estimated model is then used to estimate precipitation at unobserved locations.

This is joint work with Alexandre B. Simas and Zhen Xiong from KAUST.

High order collocation methods for fractional differential equations

Angelamaria Cardone
Department of Mathematics, University of Salerno,
via Giovanni Paolo II, n.132, I-84084 Fisciano (Sa), Italy

The numerical treatment of fractional differential equations raises a challenging issue regarding the accuracy. As a matter of fact, due to the lack of smoothness of the solution near the origin, several numerical methods exhibit low order of convergence. Spline collocation methods are able to overcome this problem, when applied on a suitable graded mesh [1, 2, 3, 4]. Within this class, we pay special attention to two-step collocation methods, which doubles the order of convergence at the same computational cost of one-step collocation methods. In this talk, we illustrate both one and two-step spline collocation methods, analyze their convergence and stability properties. In addition, we discuss their efficient MATLAB implementation and show some numerical examples. The presented results have been obtained in collaboration with Dajana Conte and Beatrice Paternoster, from University of Salerno.

References

[1] Cardone, A., Conte, D., Paternoster, B., Two-step collocation methods for fractional differential equations, *Discrete Contin. Dyn. Syst. Ser. B* **22** (2018) 1–17.

[2] Cardone, A., Conte, D., Stability analysis of spline collocation methods for fractional differential equations, *Math. Comput. Simulation* **178** (2020) 501-514.

[3] Cardone, A., Conte, D., Paternoster, B., A MATLAB implementation of spline collocation methods for fractional differential equations. *Lect. Notes Comput. Sci.*, 12949 LNCS:387–401, 2021.

[4] Pedas, A., Tamme, E., Numerical solution of nonlinear fractional differential equations by spline collocation methods, *J. Comput. Appl. Math.* **255** (2014) 216–230 .

A conservative numerical method for a time fractional diffusion equation

A. Cardone G. Frasca-Caccia
Department of Mathematics, University of Salerno
Fisciano, Via Giovanni Paolo II 132, Italy

Geometric numerical integration, the branch of numerical analysis with the goal of finding approximate solutions of differential equations that preserve some structure of the continuous problem, is a well established field of research [5].

In particular, requiring that invariants or conservation laws are preserved, on one hand, applies on the approximations some constraints that are satisfied also by the exact solutions. On the other hand, it guarantees a better propagation of the error over long integration times [3].

In the last two decades, new techniques for finding conservation laws of fractional differential equations have been derived by suitably generalising methods for PDEs [4, 6]. However, the numerical preservation of conservation laws of time fractional differential equations is a research topic still at an embryonic state.

This talk deals with the numerical solution of diffusion equations in the form

$$D_t^\alpha u = D_x^2 K(u), \qquad \alpha \in \mathbb{R},$$

where D_x is the partial derivative in space, K is an arbitrary regular function, and D_t^α denotes the Riemann-Liouville fractional derivative of order α.

The proposed numerical method combines a finite difference scheme in space with a spectral time integrator and preserves discrete versions of the conservation laws of the original differential equation [1, 2].

The conservative and convergence properties of the proposed method are verified by the computational solution of some numerical experiments.

References

[1] K. Burrage, A. Cardone, R. D'Ambrosio, B. Paternoster. *Numerical solution of time fractional diffusion systems.* Appl. Numer. Math., **116** (2017), 82–94.

[2] A. Cardone, G. Frasca-Caccia. *Numerical conservation laws of time fractional diffusion PDEs.* `arXiv.2203.01966`, (2022).

[3] A. Durán, J. M. Sanz-Serna. The numerical integration of relative equilibrium solutions. Geometric theory. *Nonlinearity*, **11**, 1547–1567, (1998).

[4] G. S. F. Frederico, D. F. M. Torres. Fractional conservation laws in optimal control theory. *Nonlinear Dyn.*, **53** (2008), 215–222.

[5] E. Hairer, C. Lubich, G. Wanner. *Geometric Numerical Integration. Structure Preserving Algorithms for Ordinary Differential Equations*, volume 31 of Springer Series in Computational Mathematics. Springer, Berlin, second edition, 2006.

[6] S. Y. Lukashchuk. Conservation laws for time-fractional subdiffusion and diffusion-wave equations. *Nonlinear Dyn.*, **80** (2015), 791–802.

Impact of the grafting topology on the geometry and dynamics of the prospective Parkinson inhibitor MCoCP4

Yadi Cheng[1], Xubiao Peng[1*], Peicho Petkov[2], Nevena Ilieva[3]

[1] School of Physics, Beijing Institute of Technology, Beijing, China
[2] Faculty of Physics, Sofia University "St. Kl. Ohridski", Sofia, Bulgaria
[3] Institute of Information and Communication Technologies, Bulgarian Academy of Sciences, Sofia, Bulgaria

Cyclotides are small peptides (28-37 amino acid residues) isolated from some plants and characterized by a cyclic peptide backbone and three interconnected stabilizing disulfide bonds – the cyclic cystine knot (CCK) motif [1]. They exhibit a wide range of biological activities, including anti-HIV, insecticidal, antitumor, antifouling, antimicrobial, hemolytic, neurotensin antagonisms, trypsin inhibition and uterotonic activities. The cyclic nature and the knotted topology of cylotides explain their conformational stability, temperature resistance, as well as their resistance to proteolytic degradation which allows them to survive when heated, as well as in the gastrointestinal tract. This helps them to maintain their activity when taken orally – a property almost unique in the world of peptides and proteins.

The range of potential applications of cyclotides is further expanded with the possibility of using them as a stabilizing skeletal construct of other biologically active epitopes [2]. An inspiring example is the engineered bioactive cyclotide MCoCP4, obtained by grafting a linearized derivative from the cyclic peptide CP4 (SLATWAVG) in loop 6 of the cyclotide MCoTI-II (PDB ID 1IB9), which was shown to reduce the α-synuclein toxicity in yeast and animal models [3, 5], accounting for characteristic aspects of the pathogenesis of Parkinson's disease. This makes MCoCP4 a promising reference point in the process of drug design. However, there is a controversy about the dynamic consequences of the grafting procedure. In particular, crystallographic data indicates reduced dynamics in loop 1, which engages the trypsin active site, upon trypsin binding, in odds with the NMR data, and a computational study suggests the emergence of a new intermediate conformation, which facilitates this binding [4].

In the present study, we take a systematic approach in analyzing the implications on the geometry and dynamics of topologically non-trivial biomolecules undergoing a grafting

*xubiaopeng@bit.edu.cn

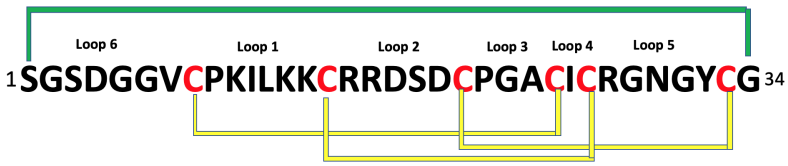

Figure 1: The primary structure of MCoCI-II (PDB ID 1IB9).

procedure by engineering virtual mimics of the investigated Parkinson inhibitor MCoCP4, with different grafting topologies: in addition to the original one, with a replacement at position 4 in loop 6, we probe grafting topologies with replacements at positions 10, 18, and 22, respectively in loops 1, 2, and 3 (Fig.1). These three representative topologies were chosen to cover charge and position variability, and to avoid possible steric clashes. The grafting in loop 1 confers a decrease in the net charge of the molecule by +1 unit, the grafting in loop 2, similarly to the original scheme in loop 6, confers a net charge increase by +1 unit, and the grafting in loop 3 does not affect the overall electric charge.

Synthetic data was generated by long-scale molecular-dynamics (MD) simulations of 1 μs for each system, using the software package GROMACS 5.1.1 [6]. For analysing the local geometry of the investigated grafting topologies, the Discrete Frenet Frame (DFF) formalism (see [7] and the references therein) was applied, in which an adequate description of the protein chain is provided in terms of a complete set of variables — the generalised bond and torsion angles (κ, τ). The folding indices for the protein backbone and side chains were computed following the definitions in [8]. In studying the protein dynamics, the quality of the synthetic data was controled by a lagged RMSD analysis [9]. The conformational ensembles of the CP4 segment in the investigated grafting topologies were classified based on their geometrical specifics (Fig. 2).

We observe substantial differences in the volatility and conformational plasticity of different parts of the engineered mimics depending on the grafting position, charge distribution, and initial conformation specifics. These observations, together with those from studying the binding dynamics between the CP4 fragments and the oligomeric α-synuclein in the above grafting topologies can be used as a guidance in engineering of ther-

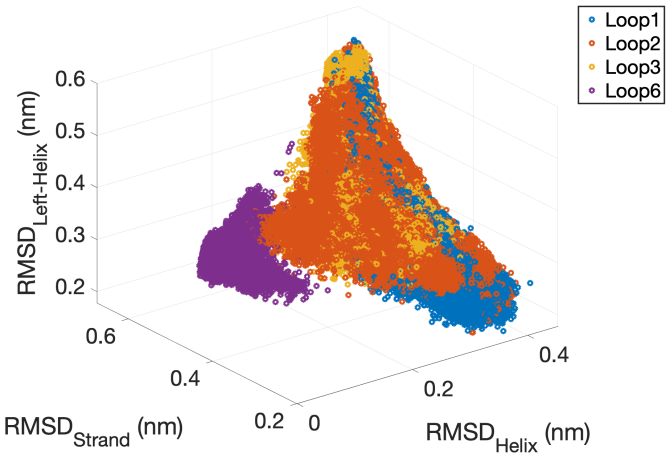

Figure 2: CP4 conformational ensembles projected onto the regular secondary-structure conformations in the investigated grafting topologies 1, 2, 3, and 6.

apeutics against Parkinson
disease, combining the efficacy of the small-molecule CP4 inhibitor with the stability and application ease of a cyclic macromolecular scaffolding.

Acknowledgements This work was supported in part by the Bulgarian National Science Fund under Grant KP-06-CN-10/2020. Computational resources were provided by the Centre for Advanced Computing and Data Processing, supported under Grant BG05M2OP001-1.001-0003 by the Science and Education for Smart Growth Operational Program (2014-2020) and co-financed by the European Union through the European structural and investment funds and at CI TASK (Centre of Informatics – Tricity Academic Supercomputer & networK), Gdansk (Poland).

References

[1] Craik, D.J., Daly, N.L., Bond, T., and Waine, C. (1999). Plant cyclotides: a unique family of cyclic and knotted proteins that defines the cyclic cystine knot structural motif. Journal of Molecular Biology **294** (1999) 1327–1336.

[2] Werle, M., Schmitz, T., Huang, H.L., Wentzel, A., Kolmar, H., Bernkop-Schnürch, A. The potential of cystine-knot microproteins as novel pharmacophoric scaffolds in oral peptide drug delivery. Journal of Drug Targeting **14**(3) (2006) 137–146.

[3] Kritzer, J.A. et al.Rapid selection of cyclic peptides that reduce α-synuclein toxicity in yeast and animal models. Nature Chemical Biology **5** (2009) 655–663.

[4] Jones, P.M. & George, A.M. Computational analysis of the MCoTI-II plant defence knottin reveals a novel intermediate conformation that facilitates trypsin binding. Scientific Reports **6** (2016) 23174.

[5] Jagadish, K., Gould, A., Borra, R., Majumder, S., Mushtaq, Z., Shekhtman, A., and Camarero, J.A. (2015). Recombinant Expression and Phenotypic Screening of a Bioactive Cyclotide Against α-Synuclein-Induced Cytotoxicity in Baker's Yeast. Angew. Chem. Int. Ed. Engl. **54**(29) (2015) 8390–8394.

[6] Abraham, M., Murtola, T., Schulz, R., Páll, S., Smith, J.C., Hess, B., and Lindahl, E. GROMACS: High performance molecular simulations through multi-level parallelism from laptops to supercomputers. SoftwareX **1** (2015) 19–25.

[7] Krokhotin, A., Niemi, A., and Peng, X. Soliton concepts and protein structure. Physical Review. E **85** (2012) 031906.

[8] Dai, J., Niemi, A.J., He, J., Sieradzan, A., and Ilieva, N. Bloch spin waves and emergent structure in protein folding with HIV envelope glycoprotein as an example. Physical Review E **93** (2016) 032409.

[9] Schreiner, W., Karch, R., Knapp, B., and Ilieva, N. Relaxation Estimation of RMSD in Molecular Dynamics Immunosimulations. Computational and Mathematical Methods in Medicine, Vol. 2012, Art. ID 173521.

On stability, convergence and scalability analysis of parallel algorithms for solution of parabolic problems with fractional power elliptic operators

Raimondas Čiegis and Ignas Dapšys
Vilnius Gediminas technical university
Saulėtekio av. 11, Vilnius, Lithuania
e-mail: rc@vgtu.lt

1 Problem Formulation

Let H be a Hilbert space with a scalar product (u, v) for $u, v \in H$. Then the L_2 norm is defined as $\|u\| = (u, u)^{1/2}$.

Let A be a self-adjoint positive definite operator

$$A: \quad H \to H, \quad A = A^*, \quad A \geq cI, \quad c > 0,$$

where I is the identity operator. Next we define a fractional power of this operator A^α with a fractional parameter $0 < \alpha < 1$. This definition can be done in a non-unique way and we use the spectral approach. Let us solve the standard eigen-problem

$$A\psi_j = \lambda_j \psi_j, \quad j = 1, 2, \ldots.$$

All eigenvalues are positive. A nonlocal operator A^α with fractional parameter $0 < \alpha < 1$ is defined as $A^\alpha u = \sum_{j=1}^{\infty} \lambda_j^\alpha (u, \psi_j)\psi_j$.

We solve the following Cauchy problem:

$$\frac{\partial u}{\partial t} + A^\alpha u = F, \quad 0 < t \leq T, \quad u(0) = u_0, \; u_0 \in H. \tag{1}$$

This presentation is a continuation of analysis started in [1, 2]. The construction of discrete schemes, the stability and convergence analysis are done in four steps. They define a general framework of our theoretical analysis.

In the **first step** we approximate operator A^α by considering a finite-dimensional Hilbert space H_h. For simplicity we denote a scalar product in H_h again as (U, V), for $U, V \in H_h$. By taking into account the spectral definition of the nonlocal operator A^α,

we approximate the local operator A by applying the finite-volume or the finite-element methods. It is required to guarantee that A_h is again a self-adjoint positive definite operator

$$A_h: \quad H_h \to H_h, \quad A_h = A_h^*, \quad A_h \geq cI_h, \quad c > 0,$$

where I_h is the discrete identity operator. The accuracy of approximation of nonlocal operator A^α by A_h^α can't be estimated in a classical and popular way when the Taylor series technique is used. It is recommended to base this analysis on the approximation accuracy of the discrete eigenvalue problem

$$A_h \psi_{hj} = \mu_j \psi_{hj}, \quad j = 1, \ldots, J.$$

In the **second** step, the semi-discrete problem is approximated by some classical discrete scheme, e.g. the Backward Euler (BE) scheme

$$\frac{U^n - U^{n-1}}{\tau} + A_h^\alpha U^n = F^n, \quad n = 1, \ldots, N, \quad U^0 = U_0. \tag{2}$$

Lemma 1. *If a solution of the problem* (1) *is sufficiently smooth, then the approximation error of BE scheme* (2) *is of order* $O(\tau)$.

The proof is standard and it is based on Taylor series technique. The stability analysis of scheme (2) is also simple and it can be done by using the Fourier or energy techniques.

Lemma 2. *The BE scheme* (2) *is unconditionally stable.*

$$\|U^n\| \leq \|U_0\| + \tau \sum_{k=1}^{n} \|F^k\|.$$

In the **third** step, we construct fully discrete schemes, they are based on rational approximations. We can write the BE scheme (2) in the following form

$$U^n = (I_h + \tau A_h^\alpha)^{-1}(U^{n-1} + \tau F^n).$$

The next step is general, when we approximate the nonlocal operator $(I_h + \tau A_h^\alpha)^{-1}$ by some local rational operator $(I_h + \tau A_h^\alpha)^{-1} \approx r_m(A_h)$. As example, we use BURA-BRASIL scheme, where the approximation of the best uniform rational approximation is constructed by using the BRASIL algorithm [3]. Then the following scheme is constructed

$$V^n = r_m(A_h)\big(V^{n-1} + \tau F^n\big), \quad n = 1, 2, \ldots, N, \quad V^0 = U_0. \tag{3}$$

First we investigate the stability of scheme (3). Note, that

$$\|I_h + \tau A_h^\alpha)^{-1}\| \leq \frac{1}{1 + \tau \mu_1^\alpha} \leq 1 - \tau \mu_1^\alpha.$$

Let m is sufficiently large in order to satisfy the estimate

$$\left|(1+\tau z^{\alpha})^{-1} - r_m(z)\right| \le \tau\mu_1^{\alpha}, \quad \forall z \in [\mu_1, \mu_J],$$

Then we get the required stability inequality.

The approximation error of the third step is computed directly by using the spectral accuracy of rational operator $r_m(A_h)$. As a second example we use URA-BRASIL type scheme.

In the last, **fourth** step parallel algorithms are used to solve the obtained systems of elliptic equations efficiently.

References

[1] R. Čiegis, R. Čiegis, I. Dapšys. A comparison of discrete schemes for numerical solution of parabolic problems with fractional power elliptic operators. Mathematics, **9** 1344 (2021) DOI:10.3390/math9121344

[2] Raim. Čiegis, I. Dapšys, Rem. Čiegis. A comparison of parallel algorithms for numerical solution of parabolic problems with fractional power elliptic operators. Axioms. 2022, 11 (3), 98 doi:10.3390/axioms11030098

[3] C. Hofreither. An algorithm for best rational approximation based on barycentric rational interpolation. Numerical Algorithms, 2021. doi: 10.1007/s11075-020-01042-0

Numerical treatment and analysis for a class of multi-term time-fractional Burgers-type equations

Neetu Garg, A.S.V. Ravi Kanth
Department of Mathematics, National Institute of Technology
Kurukshetra-136119, India

Abstract

In this work, we present numerical treatment and analysis for a class of multi-term time-fractional Burgers-type equations involving the Caputo derivative. The proposed method consists of temporal discretization using the $L2$ formula and spatial discretization using the exponential B-splines. The semi-implicit approach is applied to discretize the nonlinear term. The Von-Neumann method is utilized for stability analysis. We also present the convergence analysis. Numerical examples are solved to validate the capability of the proposed method. Comparisons with the recent works confirm the efficiency and robustness of the proposed method.

BURA(q, α, k) Preconditioning in Multiscale and Multiphysics Problems

S. Harizanov, I. Lirkov, S. Margenov
Institute of Information and Communication Technologies
Bulgarian Academy of Sciences

1 Introduction

Processes in porous media with inclusions are vital for various natural and artificial materials. In the context of this study, the flow in fractured porous media is a typical example of a non-local process, which naturally connects the problems under consideration with fractional diffusion operators. Here we use some recent advances in numerical methods for fractional diffusion problems [2]. The presented results are in the spirit of [3], generalizing the idea of using rational approximations in robust preconditioning of multiphysics problems. The application of the BURA method for fractional diffusion-reaction problems developed in [4], allows us to extend the theory from [3] to a wider class of block-diagonal preconditioners for the related coupled saddle-point systems. It may be surprising that, for $\alpha \in (0,1)$, $q \geq 0$, the matrix-vector multiplication by $\mathbb{A}^\alpha + q\mathbb{I}$ is a more difficult task to solve than solving the linear system $(\mathbb{A}^\alpha + q\mathbb{I})\mathbf{u} = \mathbf{f}$.

2 Block-diagonal preconditioning of saddle-point problems

Examples of multiphysics and multiscale problems that involve interface coupling through manifolds of lower dimensions are considered in [1, 5], see also the references therein. After a proper discretization (e.g., by the method of finite elements) such models lead to systems of linear equations with saddle-point matrices. We consider two kinds of block-diagonal preconditioners depending on the sign of the fractional powers $\alpha \in (0,1)$ and $\beta \in (-1,0)$:

$$\mathbb{C}_{q,\alpha} = Diag\left[\mathbb{A}_1, \mathbb{A}_2, \cdots, \mathbb{A}_{n_\alpha}, (\mathbb{A}_{\Delta,\Gamma} + q\mathbb{I}_\Gamma)^\alpha\right],$$

$$\mathbb{C}_{q,\beta} = Diag\left[\mathbb{B}_1, \mathbb{B}_2, \cdots, \mathbb{B}_{n_\beta}, (\mathbb{B}_{\Delta,\Gamma} + q\mathbb{I}_\Gamma)^\beta\right].$$

We assume that in both cases optimal condition number estimates hold. The first n_α blocks of $\mathbb{C}_{q,\alpha}$, respectively the first n_β blocks of $\mathbb{C}_{q,\beta}$, are sparse, symmetric and positive definite. The last blocks are fractional. thus nonlocal. They act on the sub-vectors corresponding

to the mesh points from the interface Γ, where in particular $\mathbb{A}_{\Delta,\Gamma}$ and $\mathbb{B}_{\Delta,\Gamma}$ stand for the related discrete Laplacians. Therefore, the challenging problem in implementation of the introduced block-diagonal preconditioners concerns the last blocks only.

3 BURA based preconditioners

Let us denote by $r_{q,\alpha,k}$ the best uniform rational approximation (BURA) of degree k of $z^\alpha/(1+qz^\alpha)$, $z \in [0,1]$, and let $E_{q,\alpha,k}$ be the corresponding sup-error. Following [2, 4], we generalize the definitions of BURA based preconditioners introduced in [3] from $q=0$ to the case $q \neq 0$ in the form:

$$\begin{aligned}
\left(\mathbb{C}^{BURA}_{\alpha,k}(\mathbb{A}_{\Delta,\Gamma}+q\mathbb{I}_\Gamma)\right)^{-1} &= \lambda_{1,h}^{-\alpha} r_{q,\alpha,k}(\lambda_{1,h}\mathbb{A}^{-1}_{\Delta,\Gamma}), && \alpha \in (0,1);\\
\left(\mathbb{C}^{BURA}_{\beta,k}(\mathbb{B}_{\Delta,\Gamma}+q\mathbb{I}_\Gamma)\right)^{-1} &= \mathbb{B}\lambda_{1,h}^{-(1+\beta)} r_{q,1+\beta,k}(\lambda_{1,h}\mathbb{B}^{-1}_{\Delta,\Gamma}), && \beta \in (-1,0).
\end{aligned}$$

In this way we obtain the block-diagonal preconditioners:

$$\mathbb{C}^{BURA}_{q,\alpha} = Diag\left[\mathbb{A}_1, \mathbb{A}_2, \cdots, \mathbb{A}_{n_\alpha}, \mathbb{C}^{BURA}_{\alpha,k}(\mathbb{A}_{\Delta,\Gamma}+q\mathbb{I}_\Gamma)\right],$$

$$\mathbb{C}^{BURA}_{q,\beta} = Diag\left[\mathbb{B}_1, \mathbb{B}_2, \cdots, \mathbb{B}_{n_\beta}, \mathbb{C}^{BURA}_{\beta,k}(\mathbb{B}_{\Delta,\Gamma}+q\mathbb{I}_\Gamma)\right].$$

4 Condition number estimates

The next lemmas characterize the convergence of proposed preconditioners.

Lemma 1. *Assume that the BURA degree k is large enough so that $\kappa^\alpha(\mathbb{A}_{\Delta,\Gamma}+q\mathbb{I}_\Gamma) < E^{-1}_{0,\alpha,k}$. Then, the following condition number estimate for the preconditioner $C^{BURA}_{\alpha,k}$, $\alpha \in (0,1)$, holds true*

$$\kappa\left(\left(\mathbb{C}^{BURA}_{\alpha,k}(\mathbb{A}_{\Delta,\Gamma}+q\mathbb{I}_\Gamma)\right)^{-1}(\mathbb{A}_{\Delta,\Gamma}+q\mathbb{I}_\Gamma)^\alpha\right) \leq \frac{1+E_{q,\alpha,k}\ \kappa^\alpha(\mathbb{A}_{\Delta,\Gamma}+q\mathbb{I}_\Gamma)}{1-E_{q,\alpha,k}\ \kappa^\alpha(\mathbb{A}_{\Delta,\Gamma}+q\mathbb{I}_\Gamma)}.$$

Lemma 2. *Assume that the BURA degree k is large enough so that $\kappa^{1+\beta}(\mathbb{B}_{\Delta,\Gamma}+q\mathbb{I}_\Gamma) < E^{-1}_{0,1+\beta,k}$. Then, the following condition number estimate for the preconditioner $C^{BURA}_{\beta,k}$, $\beta \in (-1,0)$, holds true*

$$\kappa\left(\left(\mathbb{C}^{BURA}_{\beta,k}(\mathbb{B}_{\Delta,\Gamma}+q\mathbb{I}_\Gamma)\right)^{-1}(\mathbb{B}_{\Delta,\Gamma}+q\mathbb{I}_\Gamma)^\beta\right) \leq \frac{1+E_{q,1+\beta,k}\ \kappa^{1+\beta}(\mathbb{B}_{\Delta,\Gamma}+q\mathbb{I}_\Gamma)}{1-E_{q,1+\beta,k}\ \kappa^{1+\beta}(\mathbb{B}_{\Delta,\Gamma}+q\mathbb{I}_\Gamma)}.$$

The proves of both lemmas are based on arguments similar to those, used in [3, Lemmas 1 – 2].

5 Concluding remarks

The block-diagonal preconditioners $\mathbb{C}_{q,\alpha}^{BURA}$ and $\mathbb{C}_{q,\beta}^{BURA}$ have optimal computational complexity. This follows from the asymptotic estimates of Lemmas 1 and 2. The numerical study of $\kappa\left(\left(\mathbb{C}_{\alpha,k}^{BURA}(\mathbb{A}_{\Delta,\Gamma}+q\mathbb{I}_{\Gamma})\right)^{-1}(\mathbb{A}_{\Delta,\Gamma}+q\mathbb{I}_{\Gamma})^{\alpha}\right)$ and $\kappa\left(\left(\mathbb{C}_{\beta,k}^{BURA}(\mathbb{B}_{\Delta,\Gamma}+q\mathbb{I}_{\Gamma})\right)^{-1}(\mathbb{B}_{\Delta,\Gamma}+q\mathbb{I}_{\Gamma})^{\beta}\right)$ for smaller k is also very important. We show that degrees of rational approximation like $k \in \{4,5,6\}$ are practically sufficient to ensure high quality BURA preconditioning.

Acknowledgments

We acknowledge the provided access to the e-infrastructure and support by the Grant No BG05M2OP001-1.001-0003, financed by the Science and Education for Smart Growth Operational Program (2014-2020) and co-financed by the European Union through the European structural and Investment funds. The work has been partially supported by the Bulgarian National Science Fund under grant No. BNSF-DN12/1.

References

[1] Bærland, T., Kuchta, M., Mardal, K-A.: Multigrid methods for discrete fractional Sobolev spaces, SIAM J. Sci. Comput. **41(2)**. A948–A972 (2019)

[2] Harizanov, S., Lazarov, R., Margenov, S.: A survey on numerical methods for spectral space-fractional diffusion problems. Fractional Calculus and Applied Analysis. **23** (6). 1605–1646 (2020)

[3] Harizanov, S., Lirkov, I., Margenov S.: Rational Approximations in Robust Preconditioning of Multiphysics Problems, *Mathematics*. **10** (2022), 780, https://doi.org/10.3390/math10050780

[4] Harizanov, S., Lazarov, R., Margenov S., Marinov, P.: Numerical solution of fractional diffusion-reaction problems based on BURA. Computers & Mathematics with Applications. **80** (2). 316–331 (2020)

[5] Kuchta, M., Laurino, F., Mardal, K., Zunino, P.: Analysis and Approximation of Mixed-Dimensional PDEs on 3D-1D Domdins Coupled with Lagrange Multipliers. SIAM J. Numer. Anal. **(59)** 1. 558–582 (2021)

Rational approximation methods with arbitrary degrees of numerator and denominator

Clemens Hofreither (RICAM)

It is by now well understood that rational approximation methods are a powerful tool for the numerical solution of spectral fractional diffusion equations, both for fractional-in-space and fractional-in-time settings. In particular, best uniform rational approximations of functions such as $x^{-\alpha}$ often lead to best-in-class numerical methods in various situations.

Within this class, most efforts have been focused on "diagonal" rational approximations where the degree of the numerator and the denominator are equal. When applying such rational approximations to a discretization of a fractional problem, the number of poles (that is, the denominator degree) corresponds to the number of applications of the inverse matrix that are required. These inversions are generally more expensive than the application of the sparse forward operator, even in the presence of optimal solvers. Therefore, it may be of interest to study rational approximations where the degree of the numerator is higher than that of the denominator, which essentially corresponds to the application of an additional matrix polynomial to the right-hand side, which is relatively cheap.

Best rational approximations of diagonal type have been very successfully computed using the BRASIL algorithm, which was also presented at the previous instalment of this workshop. However, this algorithm rapidly loses robustness as we depart from the diagonal case. Therefore, in this presentation we discuss a new Newton's method for best uniform rational approximation which can deal with arbitrary degrees.

The new algorithm is based on a formulation of the problem as a nonlinear system of equations and barycentric interpolation. We derive a closed form for the Jacobian of the system of equations and formulate a Newton's method for its solution. The resulting method for best uniform rational approximation typically converges globally and exhibits superlinear convergence in a neighborhood of the solution. Interesting auxiliary results include formulae for the derivatives of barycentric rational interpolants with respect to the interpolation nodes, and for the derivative of the nullspace of a full-rank matrix.

Using this new algorithm as a tool, we then explore best approximation errors of functions of interest in the nondiagonal rational setting and ramifications for the numerical solution of spectral fractional diffusion equations.

Kinetic Monte-Carlo Modeling of the Effects of the Stress Field generated by 1/2[111] Screw Dislocations on Carbon Diffusion in bcc Iron

I. H. Katzarov[1*], N. Ilieva[2], L. B. Drenchev[1]

[1] Institute of Metal Sciense, Equipment and Technology "Acad. A. Balevski", Bulgarian Academy of Sciences

[2] Institute of Information and Communication Technologies, Bulgarian Academy of Sciences

In this work we develop an atomistic kinetic Monte-Carlo model describing carbon diffusion in the non-homogeneous stress field created by a 1/2[111] screw dislocation in bcc-iron, where the behaviour of individual atoms is explicitly taken into account. This kMC model allows us to study both the diffusing carbon residing in the dislocation core, and carbon atoms which move through the interstitial sites in dislocation surroundings.

In the present study we use carbon migration energy barriers in the vicinity of a 1/2[111] screw dislocation in bcc iron calculated in [1]. The energetic profile of a carbon atom around a screw dislocation was determined by employing the EAM potential [2] and the nudged elastic band (NEB) technique [3]. The NEB method allows to determine the MEP of a carbon atom jumping from one binding site in the vicinity of the dislocation to another one in the neighbourhood of the original site. We employ the present kMC model to simulate carbon diffusion, trapping and detrapping in the stress field generated by a screw dislocation.

By performing long-scale carbon diffusion simulations we study the formation of carbon Cottrell atmospheres [4] around screw dislocations at different temperatures and background carbon concentrations. The kMC simulations allow us to predict the rate of formation and strength of carbon atmospheres which control the dislocations behaviour resulting in dynamic strain ageing in steel. Snapshots of the spatial distribution of carbon atoms in $10 \times 10 \times 1$ nm^3 volume during formation of the Cottrell atmosphere around screw dislocation are shown in Fig. 1.

The kMC approach, which explicitly accounts for the behaviour of individual carbon atoms, offers an atomistic view of carbon drag mechanism by which mobile dislocations can collect and transport carbon within their cores. Due to the strong attractive carbon

*email: ivaylo.katsarov@kcl.ac.uk

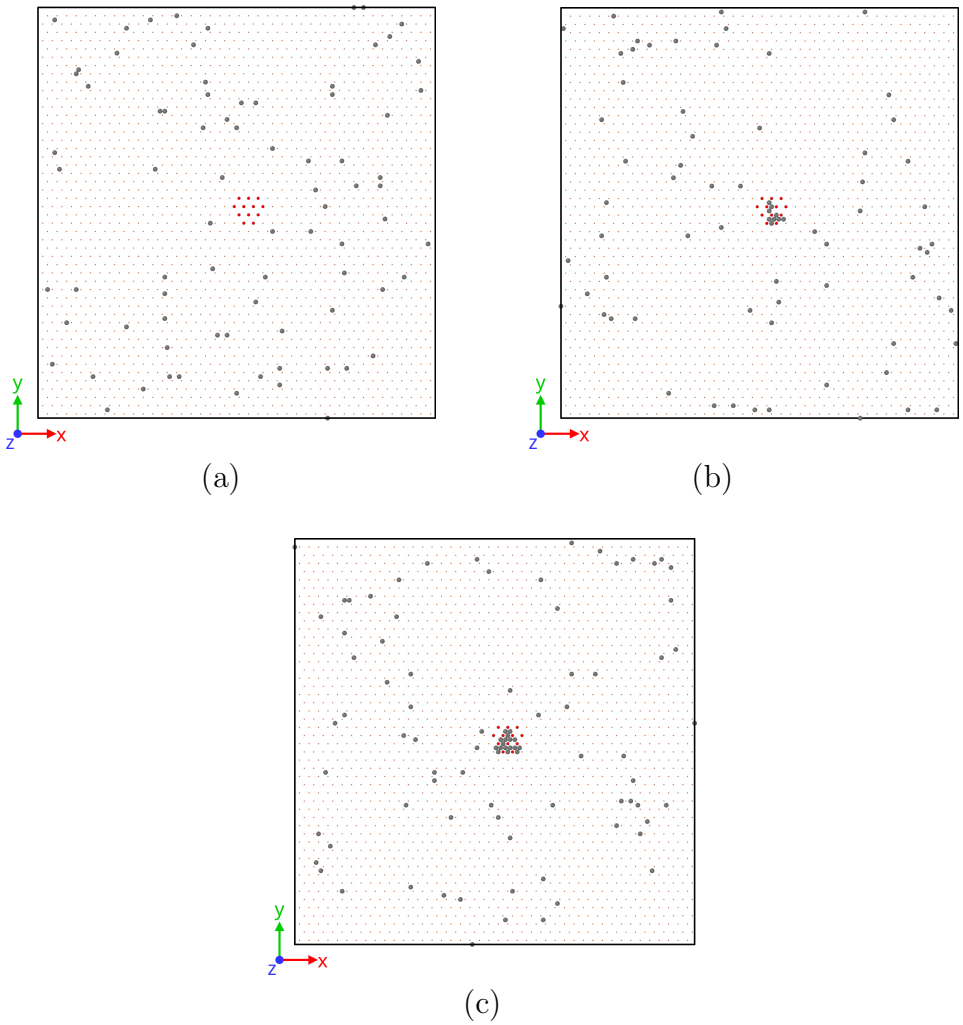

Figure 1: The formation of a carbon Cottrell atmosphere illustrated by a series of snapshots. The kMC simulations are carried out at a background carbon concentration of 0.85% and temperature 300K. The simulation cell is oriented as X=[112], Y=[110] and Z=[111]. The red coloured iron atoms designate the core region.

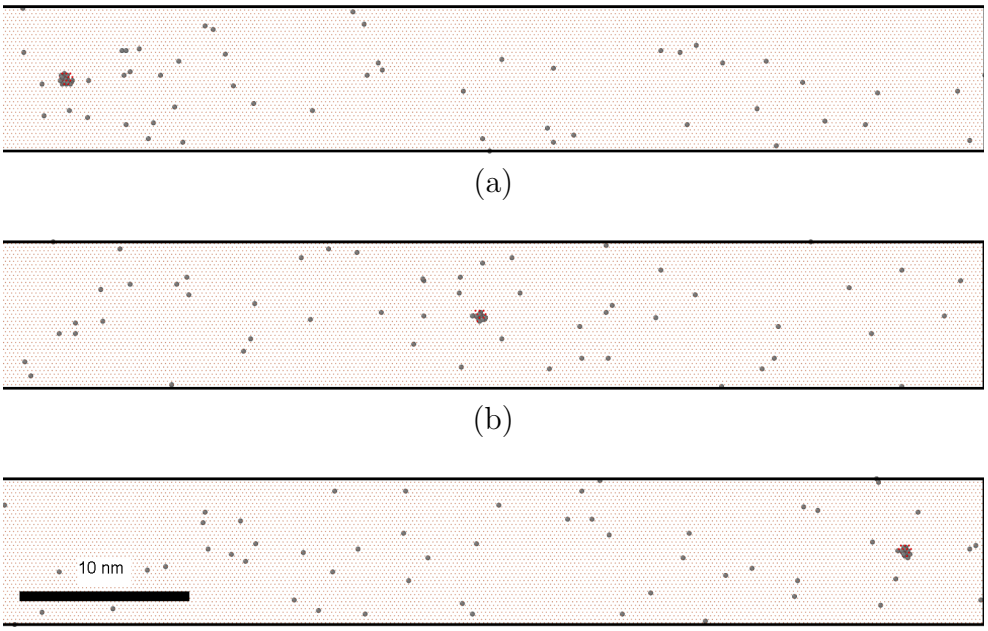

Figure 2: The motion of a screw dislocation dragging carbon ilustrated by a series of snapshots. KMC simulations are carried out at dislocation velocity $v_{dis} = 0.1$ nm/s and temperature 400 K.

binding region in the core it is in principle possible for screw dislocations to collect carbon atoms and to redistribute them. In order to be able to follow the dislocation, the carbon atoms trapped in the core need to diffuse at least as fast as the dislocation moves. Here we estimate the velocity with which a carbon atmosphere can follow a moving dislocation. Within our kMC model, we are able to simulate the migration behaviour at experimentally relevant time scales. The kMC treatment of the carbon drag mechanism presented in this work considers the evolution of the carbon cloud dragged by a mobile straight screw dislocation inside a fixed volume parallelepipedal region $60 \times 10 \times 10$ nm^3. At the starting time $t = 0$, the carbon atoms segregated to form an atmosphere around the 1/2[111] screw dislocation are at equilibrium with the background carbon concentration. We employ the kMC model to simulate the redistribution of carbon atoms when dislocation migrates in the [110] glide plane with constant velocity $v_{\rm dis}$. We simulate the carbon drag mechanism at different temperatures, background carbon concentrations and dislocation velocities and estimate the maximal dislocation velocity at which the atmosphere of carbon atoms can follow a moving screw dislocation. Carbon atoms trapped in the core can follow the dislocation if it glides slowly and viscously via a Peierls mechanism, namely the process of kink pair creation followed by kink migration. In particular we estimate the maximal dislocation velocity $v_{\rm max}$ at which the atmosphere of carbon atoms can follow a moving screw dislocation. At lower dislocation velocities the carbon atoms have sufficient time

to follow the dislocation even at lower temperatures. At higher temperatures carbon has a sufficiently high mobility to keep up with faster dislocations (Fig. 2). We consider $v_{\max}(T, c_C)$ as a limit above which screw dislocations break away from the carbon clouds and can not glide slowly and viscously. The average velocities of the dislocations gliding via a high-temperature Peierls mechanism, experimentally observed in [5], are in the range $(0, v_{\max}(T, c_C))$ predicted by our kMC model.

Acknowledgements

This research was supported in part by the Bulgarian Science Fund under the National Scientific Program "Petar Beron i NIE" (Project UMeLaMP) and under Grant KP-06-N27/19/2018, and by the European Regional Development Fund, within the Operational Programme "Science and Education for Smart Growth 2014–2020" under the Project CoE "National centre of mechatronics and clean technologies" BG05M20P001-1.001-0008-C01. Computational resources were provided by the Centre for Advanced Computing and Data Processing, supported under Grant BG05M2OP001-1.001-0003 by the Science and Education for Smart Growth Operational Program (2014-2020) and co-financed by the European Union through the European structural and investment funds.

References

[1] Gh. Ali Nematollahi, Blazej Grabowski, Dierk Raabe, Joerg Neugebauer, Multiscale description of carbon-supersaturated ferrite in severely drawn pearlitic wires, Acta Materialia **111** (2016) 321–334.

[2] C. S. Becquart, J. M. Raulot, G. Bencteux, C. Domain, M. Perez, S. Garruchet, H. Nguyen, Atomistic modeling of an Fe system with a small concentration of C, Comput. Mater. Sci. **40** (2007) 119–129.

[3] G. Henkelman, and H. Jónsson, Improved tangent estimate in the nudged elastic band method for finding minimum energy paths and saddle points. J. Chem. Phys. **113** (2000) 9978–9985.

[4] A.H. Cottrell, B.A. Bilby, Dislocation theory of yielding and strain ageing of iron, Proc. Phys. Soc. Sect. A **62** (1949) 49–62.

[5] D. Caillard, Dynamic strain ageing in iron alloys: The shielding effect of carbon, Acta Mater. **112** (2016) 273–284.

Images of special functions under generalized fractional calculus' integrals and derivatives

Virginia Kiryakova
Institute of Mathematics and Informatics, Bulgarian Academy of Sciences

Many events and phenomena in the physical and social world happen to be better modelled by equations and systems involving operators of Fractional Calculus (FC), that is integral and differential operators of fractional order. In the cases when such problems can be resolved analytically, their explicit solutions appear as the so-called Special Functions (SF) of FC. Under this notion, we mean generally the Fox H-functions and the Wright generalized hypergeometric functions ${}_p\Psi_q$, although the most popular ones are the Mittag-Leffler function $E_{\alpha,\beta}$ and its multi-indices extensions $E^{(\gamma_1,\dots,\gamma_m)}_{(\alpha_1,\dots,\alpha_m),(\beta_1,\dots,\beta_m)}$. In cases of higher integer order models, we have the simpler Meijer G-funcions, the ${}_pF_q$-functions and all their particular cases known as SF of Mathematical Physics, or "Named" SF. More details about these classes of SF can be found in the recent survey [12], and previous works as [2], [3], [4], [5].

The analyical resolution of fractional order equations is essentially based on use of integral transforms as of the Mellin- (see in [10]) and Laplace-type (see in [1]), and on the knowledge for the images of the mentioned special functions under the operators of classical FC and also of Generalized FC (GFC), in the sense of [1] and [9].

This topic, evaluation of images of special functions under operators of FC, became very hot with hundreds of recently published papers, their number growing daily. There is a flood of results for various operators of fractional order integration and differentiation and their generalizations of different special (and elementary) functions. This is natural because there is a great variety of special functions and also of operators of (classical and generalized) fractional calculus. Aside from missing an unified approach, most of these publications use same formal and standard procedures, and often the results sound not of practical use, because the final results are either in terms of different kind of special function, or are not recognized as known special functions, or have not enough visible form.

In a series of older and very recent works (mentioned in the list below) we have presented an unified approach to do the mentioned task at once and in well visible form, for both operators of generalized fractional calculus and all generalized hypergeometric functions ${}_p\Psi_q$ and ${}_pF_q$, thus incorporating most of the special (and elementary) functions. In this way, great part of the results in the mentioned publications are well predicted and appear as very particular cases, [6].

For example, we provide clear and shortly written results for operators of GFC (involving compositions of Riemann–Liouville, Erdélyi-Kober, Saigo, Marichev-Saigo-Maeda, hyper-Bessel and generalized Gel'fond-Leont'ev operators, etc.) of the H-functions and ${}_p\Psi_q$-functions in general (including the variety of mentioned SF of FC and "clasical" SF and elementary functions).

The proposed general scheme is based on some few basic classical results, combined and extended with ideas and developments from the author's research, surveyed recently in Kiryakova [6], [7], [8], [11], [12].

References

[1] V. Kiryakova, *Generalized Fractional Calculus and Applications*, Longman–J. Wiley, Harlow–N. York, 1994;

[2] V. Kiryakova, All the special functions are fractional differintegrals of elementary functions. *J. Phys. A: Math. & General* **30** (1997), 5085-5103, doi:10.1088/0305-4470/30/14/019;

[3] V. Kiryakova, Multiple (multiindex) Mittag-Leffler functions and relations to generalized fractional calculus. *J. Comput. Appl. Math.* **118** (2000), 241–259, 2000, doi:10.1016/S0377-0427(00)00292-2;

[4] V. Kiryakova, The special functions of fractional calculus as generalized fractional calculus operators of some basic functions. *Computers and Math. with Appl.* **59** (2010), 1128-1141, doi:10.1016/j.camwa.2009.05.014;

[5] V. Kiryakova, The multi-index Mittag-Leffler functions as an important class of special functions of fractional calculus. *Computers and Math. with Appl.* **59** (2010), 1885-1895, doi:10.1016/j.camwa.2009.08.025;

[6] V. Kiryakova, Fractional calculus operators of special functions?–The result is well predictable!. *Chaos Solitons and Fractals* **102** (2017), 2-15, doi:10.1016/j.chaos.2017.03.006;

[7] V. Kiryakova, Commentary: 'A remark on the fractional integral operators and the image formulas of generalized Lommel-Wright function'. *Front. Phys.* (Oct. 2019), # 145, doi:10.3389/fphy.2019.00145;

[8] V. Kiryakova, Fractional calculus of some "new but *not* new special functions: K-, multi-index-, and S-analogues. *Amer. Inst. of Physics Conf. Proc.* **2172** (2019), # 0500088, doi:10.1063/1.5133527;

[9] V. Kiryakova, Generalized fractional calculus operators with special functions. In: *Handbook of Fractional Calculus with Applications. Volume 1: Basic Theory*, Ch. 4, 87-110, De Gryuter, 2019, doi:10.1515/9783110571622-004;

[10] V. Kiryakova, J. Paneva-Konovska, On the multi-index Mittag-Leffler functions and their Mellin transforms, *Intern. J. Appl. Math.* **33** (2020), 549-571, doi:10.12732/ijam.v33i4.1;

[11] V. Kiryakova, Unified approach to fractional calculus images of special functions – A survey, *Mathematics* **8** (2020), Art. ID 2260, 35 pp., doi:10.3390/math8122260;

[12] V. Kiryakova, A guide to special functions in fractional calculus, *Mathematics* **9** (2021), Art. 106, 35 pp., doi:10.3390/math9010106.

Analytical and Numerical Simulation of Atmospheric Dispersion by Subdiffusion Equations with Vertical Degeneration

Miglena N. Koleva[1], Lubin G. Vulkov[2]
[1]Department of Mathematics, FNSE, University of Ruse,
7017 Ruse, Bulgaria,
[2]Department of Applied Mathematics and Statistics,
FNSE, University of Ruse, 7017 Ruse, Bulgaria,
e-mails: mkoleva@uni-ruse.bg, lvalkov@uni-ruse.bg

Usually in the real-world simulation of the atmospheric pollution the basic feature of the phenomena could be explained by the non-stationary advection-diffusion equation [2]

$$\frac{\partial^\alpha c}{\partial t^\alpha} + v\frac{\partial c}{\partial y} - w\frac{\partial c}{\partial z} - \frac{\partial}{\partial y}\left(K_y\frac{\partial c}{\partial y}\right) - \frac{\partial}{\partial z}\left(K_z\frac{\partial c}{\partial z}\right) - qc = f(y,z,t), \tag{1}$$

where $c = c(y,z,t)$ is the average *concentration*, $\frac{\partial^\alpha u}{\partial t^\alpha}$ represents the Caputo fractional derivative ($\Gamma(\cdot)$ is Gamma function)

$$\frac{\partial^\alpha}{\partial t^\alpha} = \frac{1}{\Gamma(1-\alpha)}\int\limits_0^t \frac{\partial u(y,z,\xi)}{\partial \xi}(t-\xi)^{-\alpha}d\xi, \quad 0<\alpha<1 \ \text{ and } \ \frac{\partial u(y,z,t)}{\partial t}, \quad \alpha = 1. \tag{2}$$

The *horizontal* dimension y, $0 < y < Y$ is from hundred to several kilometers, while for the *vertical* direction $0 < z < Z$, the typical is the *diffusion degeneration* $K_z(y,0,t) = K_z(y,Z,t) = 0$. For example, according to the Monin-Obukhov theory of the atmospheric layers $K_z(y,0,t) = \varphi(t)z^\beta(Z-z)^\gamma(1-22)\frac{z}{L}$, where $L<0$ is the Monin-Obukhov length, $\varphi(t)$ is the measured friction function and $\beta,\gamma>0$ are constants.

The main goal of the present study is the analysis of the influence of the *vertical diffusion degeneration* on the propagation of the concentration $c(y,z,t)$. It is sufficient to investigate the one-dimensional model equation with ends degenerations.

$$D_0^\alpha u = k(x,t)\frac{\partial^2 u}{\partial x^2} + p(x,t)\frac{\partial u}{\partial x} + q(x,t)u + f(x,t), \ (x,t)\in Q_T = \Omega\times(0,T), \tag{3}$$

$$u(x,0) = u_0(x), \ x\in\overline{\Omega}, \ k(0,t) = 0, \ k(l,t) = 0, \ k(x,t)\geq \widetilde{k} > 0, \ x\in\Omega = (0,l). \tag{4}$$

In the first part, the analytical study discussed the maximum principle (MP) and the energy correctness of the problem (3)-(4). For time-fractional equations without degeneration, the weak maximum principle was proved by Luchko (2009) assuming negative coefficient q and this restriction on the reaction coefficient on the sign was removed by Luchko and Yamamoto (2017) and Kopteva [3]. In our case we cannot remove the restriction because of the boundary degeneration.

Lemma 1 (Maximum principle)**.** *Assume the formulation (3)-(4) holds and* $-q(x,t) \geq \widetilde{q} > 0$, $u(x,t) \in C^{2,1}(Q_T) \cap C(\overline{Q}_T)$. *If* $Lu = D_0^\alpha u - k(x,t)\frac{\partial^2 u}{\partial x^2} - p(x,t)\frac{\partial u}{\partial x} - q(x,t)u \leq 0$, *then* $u(x,t)$ *can only attain the positive maximum at the non-degenerate parabolic boundary.*

Corollary 1. *Suppose that the assumptions of Lemma 1 hold, but* $Lu \geq 0$, *then* $u(x,t)$ *only attains its negative minimum at the non-degenerate parabolic boundary.*

Theorem 2. *Suppose that the assumptions of Lemma 1 hold without of the sign of* Lu *defined. Then, for* $u(x,t)$ *we have the following estimate*

$$\max_{\overline{Q}_T} u \leq \max\left\{\frac{1}{\widetilde{q}}\sup_{Q_T}|f|, \sup_{\Omega}|u_0|\right\}.$$

We rewrite the equation (3) in the semidivergent form

$$D_0^\alpha u = \mathcal{L}u + f(x,t), \quad \mathcal{L}u = \frac{\partial}{\partial x}\left(k(x,t)\frac{\partial u}{\partial x}\right) + \left(p(x,t) - \frac{\partial k(x,t)}{\partial x}\right)\frac{\partial u}{\partial x} + q(x,t)u. \quad (5)$$

The coefficient at $\frac{\partial u}{\partial x}$ plays a crucial role at the discretization of the boundary conditions. Namely, if

$$p(0,t) - \frac{\partial k(0,t)}{\partial x} \geq 0 \ \text{ and } \ p(1,t) - \frac{\partial k(1,t)}{\partial x} \leq 0 \ \text{ for } \ t \in [0,T], \quad (6)$$

no boundary conditions can be imposed. If $p(0,t) - \frac{\partial k(0,t)}{\partial x} < 0$ for $t \in [0,T]$, a boundary conditions at $x = 0$, such as $u(0,t) = \varphi_l(t)$ for $t \in [0,T]$, must be imposed in order to have unique solution. If $p(1,t) - \frac{\partial k(1,t)}{\partial x} > 0$ for $t \in [0,T]$, a boundary conditions at $x = l$, such as $u(l,t) = \varphi_r(t)$ for $t \in [0,T]$, must be imposed. This discussion provides the well-posedness of the initial-boundary value problems, such defined.

Theorem 3. *Let* $k(x,t) \in C^{1,0}(\overline{Q}_T)$, $p(x,t)$, $q(x,t)$, $f(x,t) \in C(\overline{Q}_T)$, $k(x,t)$ *is defined in (4) and* $q(x,t) \leq 0$ *everywhere in* $\overline{Q}_T$. *If the solution as defined above exists in* $C^{2,1}(\overline{Q}_T)$, *then it is unique and stable with respect to the initial value* $u_0(x)$ *and right-hand side* $f(x,t)$ *and the boundary values of* $\phi_l(t)$ *and* $\varphi_r(t)$. *Also, the following estimate holds*

$$\|u\|_{L_2}^2(t) \leq \|u_0\|_{L^2}^2 E_\alpha(C_1 + \alpha) + \Gamma(\alpha)E_{\alpha,\alpha}(C_1 t^\alpha)D_0^{-\alpha}C_2(t),$$

where $C_1 = 1 + c_1 + c_2 + 2c_3$ *and* $C_2(t) = \int\limits_0^l f^2(x,t)dx + c_4(t)\varphi_l^2(t) + c_5(t)\varphi_r^2(t)$,

$$c_1 = \max_{(x,t)\in Q_T}\left|\tfrac{\partial^2 k(x,t)}{\partial x^2}\right|, \quad c_2 = \max_{(x,t)\in Q_T}\left|\tfrac{\partial p(x,t)}{\partial x}\right|, \quad c_3 = \max_{(x,t)\in Q_T}|q(x,t)|,$$

$$c_4 = -\min\left\{0, p(0,t) - \tfrac{\partial k(0,t)}{\partial x}\right\}, \quad c_5 = \max\left\{0, p(l,t) - \tfrac{\partial k(l,t)}{\partial x}\right\}$$

and $E_\alpha(\cdot)$, $E_{\alpha,\alpha}(\cdot)$ are Mittag-Leffler functions.

Further, on the base of (6), we construct positivity preserving numerical scheme for (5). For the discretization of the time fractional derivative we use $L1$ formula on non-uniform time grid [4]. To obtain the spatial discretization we unfold the monotonic method proposed in [1]. We extend the idea for the case, when no boundary conditions are imposed.

We introduce non-uniform spatial and temporal meshes with N and M grid nodes, respectively. Denote the numerical solution at point (x_i, t^n) by U_i^n and write the discrete equations in the form

$$L_h U_i^{n+1} = 0, \quad i = 0, 1, \ldots, M, \quad n = 0, 1, \ldots, M. \tag{7}$$

Theorem 4. *Suppose that the assumptions of Lemma 1 holds. If $L_h U_i^n \leq 0$, $i = 0, 1, \ldots, N$, $n = 0, 1, \ldots, M$, then the solution U_i^n, $i = 0, 1, \ldots, N$, $n = 0, 1, \ldots, M$ of (7) attains its positive maximum only at the non-degenerate parabolic boundary.*

Corollary 2. *If $u_0(x) \geq 0$ and $\varphi_l(t) \geq 0$, $\varphi_r(t) \geq 0$ (in the case $p(0,t) - \frac{\partial k}{\partial x}(0,t) < 0$, $p(l,t) - \frac{\partial k}{\partial x}(l,t) > 0$), then $U_i^n \geq 0$, $i = 0, 1, \ldots, M$, $n = 0, 1, \ldots, M$.*

Acknowledgements This research is supported by the Bulgarian National Science Fund under the Bilateral Project KP/Russia 06/12 "Numerical methods and algorithms in the theory and applications of classical hydrodynamics and multiphase fluids in porous media" from 2020.

References

[1] E. I. Golant, Conjugate families of difference schemes for equations of parabolic type with lowest terms, Zh. Vychisl. Mat. Mat. Fiz. 18(5), 1162–1169 (1978).

[2] A.G.O. Goulart, M.J. Lazo, J.M.S. Suarez, D.M. Moreira,Fractional derivative models for atmospheric dispersion of pollutants, Physica A:Statistical Mechanics and its Applications 477, 9–19 (2017).

[3] N. Kopteva, Maximum principle for time-fractional parabolic equations with reaction coefficient of arbitrary sign, arXiv:2202.10220v1, Feb. 2022.

[4] M. Stynes, E. O'Riordan, J.L. Gracia, Error analysis of a finite difference method on graded meshes for a time-fractional diffusion equation, SIAM J. Numer. Anal. 55(2), 1057–1079 (2017).

Pointwise-in-time a-priori and a-posteriori error control for time-fractional parabolic equations

Natalia Kopteva
Department of Mathematics and Statistics, University of Limerick
Ireland
Web page: https://staff.ul.ie/natalia/

An initial-boundary value problem with a Caputo time derivative of fractional order $\alpha \in (0,1)$ is considered, solutions of which typically exhibit a singular behaviour at an initial time. For this problem, building on some ideas from [1], we give a simple and general numerical-stability analysis using barrier functions, which yields sharp pointwise-in-time error bounds on quasi-graded temporal meshes with arbitrary degree of grading. This approach is employed in the error analysis of the L1 and Alikhanov L2-1_σ fractional-derivative operators [2], as well as an L2-type discretization of order $3-\alpha$ in time [3]. This methodology is also generalized for semilinear fractional parabolic equations [4]. In particular, our error bounds accurately predict that milder (compared to the optimal) grading yields optimal convergence rates in positive time. The theoretical findings are illustrated by numerical experiments.

Furthermore, pointwise-in-time a posteriori error bounds will be given in the spatial L_2 and L_∞ norms. Hence, an adaptive mesh construction algorithm is applied for the L1 method, which yields optimal convergence rates $2-\alpha$ in the presence of solution singularities [5, 6].

References

[1] N. Kopteva, Error analysis of the L1 method on graded and uniform meshes for a fractional-derivative problem in two and three dimensions, Math. Comp., 88 (2019), 2135–2155.

[2] N. Kopteva and X. Meng, Error analysis for a fractional-derivative parabolic problem on quasi-graded meshes using barrier functions, SIAM J. Numer. Anal., 58 (2020), 1217–1238.

[3] N. Kopteva, Error analysis of an L2-type method on graded meshes for a fractional-order parabolic problem, Math. Comp., (2020), published electronically on 14-Jul-2020; doi: 10.1090/mcom/3552.

[4] N. Kopteva, Error analysis for time-fractional semilinear parabolic equations using upper and lower solutions, SIAM J. Numer. Anal., 58 (2020), 2212–2234.

[5] N. Kopteva, Pointwise-in-time a posteriori error control for time-fractional parabolic equations, Appl. Math. Lett., 2021, https://doi.org/10.1016/j.aml.2021.107515.

[6] N. Kopteva and M. Stynes, A posteriori error analysis for variable-coefficient multiterm time-fractional subdiffusion equations, submitted for publication (Feb 2022); arXiv:2202.13357.

BURA based non-overlapping domain decomposition preconditioning

N. Kosturski, S. Margenov, Y. Vutov
Institute of Information and Communication Technologies
Bulgarian Academy of Sciences

1 Non-overlapping domain decomposition

We consider the Poisson equation $-\Delta u = f$ in the polygonal domain $\Omega \in \mathbb{R}^2$, equipped with appropriate boundary conditions on $\Gamma = \partial\Omega$. Assume that the Finite Element Method (FEM) is applied for numerical solution of the problem using linear elements on a quasi-uniform triangulation $\mathcal{T}_h$, thus obtaining the linear system $A\mathbf{u} = \mathbf{f}$.

We now assume that $\{\Omega_i\}_{i=1}^m$ is a non-overlapping partitioning of Ω with interface γ. The stiffness matrix A is written in the form

$$A = \begin{pmatrix} A_D & A_{D\gamma} \\ A_{\gamma D} & A_\gamma \end{pmatrix}, \quad A_D = blockdiag\left(A_1, A_2, \cdots, A_m\right),$$

where the blocks A_i correspond to the subdomains Ω_i, $i = 1, 2, \cdots, m$, and A_γ - to the interface. The studied multiplicative non-overlapping domain decomposition (DD) preconditioner reads as [3, 4]

$$C_{DD} = \begin{pmatrix} A_D & \\ A_{\gamma D} & \Lambda^{1/2} \end{pmatrix} \begin{pmatrix} I & A_D^{-1} A_{D\gamma} \\ & I \end{pmatrix},$$

where Λ is the discrete Laplacian corresponding to $\mathcal{T}_h \cap \gamma$. It is known that $\kappa\left(C_{DD}^{-1} A\right) = O(1)$, that is the DD preconditioner provides an optimal convergence rate. For the model problem on a regular mesh with an interface along a single mesh line, $\Lambda = tridiag(-1, 2, -1)$, and when in the PCG method FFT is used to solve the systems with $\Lambda^{1/2}$, the DD preconditioner has almost optimal complexity $O(N)$, N is the number of FEM unknowns; see, for example, the pioneering work [3] and its generalization [4]. Until recently, the implementation of the preconditioner C_{DD} in the case of general geometry of the manifold γ was a challenging problem.

2 BURA based preconditioner

Let us denote by $r_{1/2,k}$ the best uniform rational approximation of degree k of $z^{1/2}$, $z \in [0, 1]$, and let $E_{1/2,k}$ be the corresponding error [1]. It is known that $E_{1/2,k}$ decreases exponentially

with increasing k. Following [2], we consider the preconditioner $C^{BURA}_{1/2,k}(\Lambda)$ of $\Lambda^{1/2}$ defined by its inverse

$$\left(C^{BURA}_{1/2,k}(\Lambda)\right)^{-1} = \lambda_{1,h}^{-1/2} r_{1/2,k}(\lambda_{1,h}\Lambda^{-1}),$$

where $\lambda_{1,h} > 0$ is the minimal eigenvalue of Λ. Then assuming that the degree k is large enough so that $E_{1/2,k}\ \kappa^{1/2}(\Lambda) < 1$, the following condition number estimate holds

$$\kappa\left(\left(C^{BURA}_{1/2,k}(\Lambda)\right)^{-1}\Lambda^{1/2}\right) \leq \frac{1 + E_{1/2,k}\ \kappa^{1/2}(\Lambda)}{1 - E_{1/2,k}\ \kappa^{1/2}(\Lambda)}.$$

Now the proposed BURA based DD preconditioner has the form

$$C^{BURA}_{DD,k} = \begin{pmatrix} A_D & \\ A_{\gamma D} & \sigma C^{BURA}_{1/2,k,\sigma}(\Lambda) \end{pmatrix} \begin{pmatrix} I & A_D^{-1}A_{D\gamma} \\ & I \end{pmatrix},$$

where $\sigma > 0$ is a parameter, independent of the mesh size h. $C^{BURA}_{DD,k}$ is an asymptotically optimal preconditioner, i.e. it's computational complexity is $O(N)$. The estimates from [4] show that small degree k (say 3 or 4) is enough for efficient application of the method. From a practical point of view it is important that for larger N the degree k (that is the number of auxiliary linear systems with matrices which are positive diagonal perturbations of Λ) has little effect on the overall computational complexity.

3 Numerical tests

The numerical results are for a test problem in $\Omega = (0,1) \times (0,1)$, $m = 4$, and $\Omega_1 = (0, 0.5) \times (0, 0.5)$, $\Omega_2 = (0.5, 1) \times (0, 0.5)$, $\Omega_3 = (0, 0.5) \times (0.5, 1)$ and $\Omega_4 = (0.5, 1) \times (0.5, 1)$, assuming homogeneous Dirichlet boundary conditions. The right-hand side is $f(x, y) = \sin(\pi x)\sin(\pi y)$, corresponding to the solution $u(x, y) = \sin(\pi x)\sin(\pi y)/(2\pi^2)$. All matrices are obtained by linear FEM discretization on uniform mesh with a mesh parameter h. The number of Preconditioned Conjugate Gradient (PCG) iterations with the domain decomposition preconditioner $C^{BURA}_{DD,k,\sigma}$ are examined, where $k = 12$ and $\sigma = 2$.

Table 1: Number of finite elements N_e, number of unknowns N, and number of PCG iterations N_{it} with preconditioner $C^{BURA}_{DD,12,2}$: stopping criteria $\epsilon = 10^{-6}$

N_e	N	N_{it}
8 388 608	4 190 209	9
2 097 152	1 046 529	8
524 288	261 121	8
131 072	65 025	8
32 768	16 129	7

The reported results illustrate the optimal convergence rate of the proposed non-overlapping domain decomposition method.

Acknowledgements

We acknowledge the provided access to the e-infrastructure and support by the Grant No BG05M2OP001-1.001-0003, financed by the Science and Education for Smart Growth Operational Program (2014-2020) and co-financed by the European Union through the European structural and Investment funds. The work has been partially supported by the Bulgarian National Science Fund under grant No. BNSF-DN12/1.

References

[1] Harizanov, S., Lazarov, R., Margenov, S., Marinov, P., Pasciak, J.: Analysis of numerical methods for spectral fractional elliptic equations based on the best uniform rational approximation. *Journal of Computational Physics*. **408**. 109285 (2020)

[2] Harizanov, S., Lirkov, I., Margenov S.: Rational Approximations in Robust Preconditioning of Multiphysics Problems, *Mathematics*. **10** (2022), 780. https://doi.org/10.3390/

[3] Nepomnyaschikh S.V.: Mesh theorems on traces, normalizations of function traces and their inversion. *Sov J Numer Anal Math Model*. **6** (3) (1991). 223–242

[4] Nepomnyaschikh S.V.: Domain decomposition methods. *Lectures on Advanced Computational Methods in Mechanics. Radon Series on Computational and Applied Mathematics*. **1** (3) (2007). 89–158

Fractional operators in coupled multiphysics problems with implicit coupling *

Miroslav Kuchta†

Abstract

Construction of parameter robust solution algorithms for coupled multiphysics problems is challenging due to the interaction between the system components and practical applications require that the solvers perform uniformly across parameter regimes. For model formulations where the coupling is realized in terms of Lagrange multipliers, robust monolithic preconditioners are known to rely on operators in weighted fractional Sobolev spaces over the interface. In this contribution, we show that fractional order operators are crucial for robustness even in multiphysics formulations where the coupling is implicit and where no auxiliary interface variables are present.

Keywords: Robust solvers, parameter-robust preconditioning, fractional order operators

1 Introduction

In order to distinguish between the formulations with explicit/implicit coupling let us introduce an abstract multiphysics problem posed on non-overlapping domains Ω_1, Ω_2 with a common interface $\Gamma = \overline{\Omega_1} \cap \overline{\Omega_2}$. The physics in the respective subdomains is assumed to be described by operators $A_i : V_i \to V_i'$, $i = 1, 2$ while the coupling between the systems is stated in terms of the restriction operators $T_i : V_i \to Q'$. Here $V_i = V_i(\Omega_i)$ and $Q = Q(\Gamma)$ are Hilbert spaces. Alternatively, the interaction between the subsystems can be represented by the coupling operator $C : V_1 \to V_2'$. Finally, letting $u_i \in V_i$ be the unknowns in the bulk domains and $\lambda \in Q$ be the Lagrange multiplier enforcing the interface coupling, we formally define two formulations of the multiphysics problem: Given $\boldsymbol{f}_E$, respectively $\boldsymbol{f}_I$, find $\boldsymbol{u}_E := (u_1, u_2, \lambda)$, respectively $\boldsymbol{u_I} := (u_1, u_2)$, such that

$$\mathcal{A}_E \boldsymbol{u}_E := \begin{bmatrix} A_1 & 0 & T_1' \\ 0 & A_2 & T_2' \\ T_1 & T_2 & \end{bmatrix} \begin{bmatrix} u_1 \\ u_2 \\ \lambda \end{bmatrix} = \boldsymbol{f}_E, \quad \mathcal{A}_I \boldsymbol{u}_I := \begin{bmatrix} A_1 & C' \\ C & -A_2 \end{bmatrix} \begin{bmatrix} u_1 \\ u_2 \end{bmatrix} = \boldsymbol{f}_I. \tag{1}$$

*Joint work with Wietse M. Boon (wietsemarijn.boon@polimi.it), Karl Erik Holter (karl0erik@gmail.com), Martin Hornkjøl (marhorn@math.uio.no), Timo Koch (timokoch@uio.no), Kent-André Mardal (kent-and@math.uio.no), Ricardo Ruiz-Baier (ricardo.ruizbaier@monash.edu).

†Simula Research Laboratory, Oslo, Norway (miroslav@simula.no)

Due to presence of the explicit interface variable we refer to the formulation induced by operator $\mathcal{A}_E$ as having explicit coupling while $\mathcal{A}_I$ leads to the implicit coupling formulation.

We remark that the operators A_i in $\mathcal{A}_E$, $\mathcal{A}_I$ in (1), as well as the bulk variables u_i in the two formulations, are not identical in general since they typically stem from different strong formulations. For example, the (explicitly) coupled Stokes-Darcy problem [12] utilizes the Darcy formulation in terms of pressure p and flux $u := -K\nabla p$ so that $u_2 := (u, p) \in V_2 := H(\mathrm{div}, \Omega_2) \times L^2(\Omega_2)$ and

$$\langle A_2(u,p),(v,q)\rangle := \int_{\Omega_2} \left(K^{-1}u \cdot v - p\nabla\cdot v - q\nabla\cdot u\right) \,\mathrm{d}x \quad \forall (v,q) \in V_2.$$

Moreover, T_i corresponds to the normal trace operator $T_i u_i = u_i \cdot \nu$ with ν being the normal to the interface and

$$\begin{aligned}\langle A_1(u_1,p_1),(v_1,q_1)\rangle := &\int_{\Omega_1} 2\mu\epsilon(u_1) : \epsilon(v_1)\,\mathrm{d}x + \int_\Gamma \alpha_{\mathrm{BJS}}\sqrt{\tfrac{\mu}{K}} P_\nu u_1 \cdot P_\nu v_1 \,\mathrm{d}s \\ &- \int_{\Omega_1} (p_1\nabla\cdot v_1 + q_1 \nabla\cdot u_1)\,\mathrm{d}x \quad \forall (v_1,q_1) \in V_1 := H^1(\Omega_1)\times L_2(\Omega_1).\end{aligned}$$

Here, $P_\nu = \mathrm{Id} - \nu\otimes\nu$, $\epsilon = \mathrm{sym}\nabla$ and α_{BJS}, μ, K are positive coefficients. On the other hand, while using the same operator A_1, the (implicitly coupled) Stokes-Darcy problem [6] is based on the primal Darcy formulation, and in turn $u_2 := p \in V_2 := H^1(\Omega_2)$ and

$$\langle A_2 p, q\rangle := \int_{\Omega_2} K\nabla p\cdot\nabla q\,\mathrm{d}x \quad \forall q \in V_2.$$

The coupling operator is then $\langle Cu_1, q\rangle := \int_\Gamma q u_1\cdot\nu\,\mathrm{d}s$, $(u_1,q)\in V_1\times Q$.

The formulations due to $\mathcal{A}_E$, $\mathcal{A}_I$ lead to numerical methods which differ by approximation properties or properties of the discrete solution, e.g. mass conservation. Given the same triangulation of the domains Ω_i the operators also differ in their computational cost; the approaches lead to linear systems having different number of degrees of freedom which may also be more amenable to a particular solution approach. For example, parameter robust domain decomposition approaches are known for the explicit Stokes-Darcy problem [3, 7] while for the implicit formulation, robustness is limited to certain parameter regimes or requires tuning of algorithmic parameters [5]. In the following, we shall construct robust monolithic solvers for (1) in the form of preconditioned Krylov methods.

2 Monolithic preconditioners

Assuming operators A_i in (1) are self-adjoint and coercive on spaces V_i, preconditioners for the implicit/explicit formulations can be derived as Schur complement preconditioners [14]. Then, however, spectrally equivalent approximation to the Schur complement must be available and for parameter robustness the equivalence bounds must be independent of the parameters. Such approximations can be constructed by establishing well-posedness of (1)

(see [13, 9]), as the operators inducing the inner product on spaces Q for $\mathcal{A}_E$, respectively V_2 for $\mathcal{A}_I$.

For the explicit formulation the Schur complement $T_1A_1^{-1}T_1' + T_2A_2^{-1}T_2'$ is defined over the interface and from considerations about the mapping properties of the restriction operators it is natural to consider its approximations in the form $(-\alpha_1\Delta_\Gamma)^{s_1} + (-\alpha_2\Delta_\Gamma)^{s_2}$. Here, $-\Delta_\Gamma$ is the Laplace operator on the interface, the coefficients $\alpha_i > 0$ are related to model parameters while the exponents $s_i \in \mathbb{R}$ are specific to T_i, A_i and V_i, Q. Indeed, the construction in terms of the fractional Laplacian has been used to construct robust preconditioners in coupled diffusion problems [11] (therein, $s_i = -\frac{1}{2}$), coupled reduced order problems [10] (therein, $s_1 = -\frac{1}{2}$, $s_2 = -1$) or explicit Stokes-Darcy problem [8] (therein, $s_1 = -\frac{1}{2}$, $s_2 = \frac{1}{2}$). In these cases the fractional operators arise from the Lagrange multipliers being posed in intersection spaces $\alpha_1^{1/2}H^{s_1}(\Gamma) \cap \alpha_2^{1/2}H^{s_2}(\Gamma)$.

The issue with the implicit formulation $\mathcal{A}_I$ is that the Schur complement $A_2 + CA_1^{-1}C'$ now constitutes an operator in the bulk and not on the interface. Clearly, the latter summand represents a contribution due to the coupling. However, how to construct its approximation as an operator over Ω_2 is far from evident. For example, the weighted identity operator (leading to scaled mass matrix) considered in [4] does not yield robust preconditioning. In order to obtain robustness, we propose here the construction

$$A_2 + R'(-\alpha_1\Delta_\Gamma)^{s_1}R, \tag{2}$$

R being a suitable restriction operator, which attempts to reflect the role of $CA_1^{-1}C$ in the coupling.

3 Results

In our recent work [1, 2] we utilize the ansatz (2) to construct parameter robust preconditioners for coupled Stokes-Darcy and Stokes-Biot system. In particular, the construction is rigorously justified by analysis of the continuous problems where we show well-posedness with the Darcy[1] pressure controlled in the norm

$$\|p\|_{V_2}^2 := K\|\nabla p\|_{L^2(\Omega_2)}^2 + (2\mu)^{-1}\|p\|_{H^{-1/2}(\Gamma)}^2. \tag{3}$$

Note the presence of the fractional norm on the interface. The complete preconditioner for Stokes-Darcy formulation $\mathcal{A}_I$ is then a diagonal operator

$$\mathcal{B}_I = \begin{bmatrix} -\nabla\cdot(2\mu\epsilon) + \alpha_{\mathrm{BJS}}P\nu' P_\nu & & \\ & (1/(2\mu))I & \\ & & -K\Delta_{\Omega_2} + (-\frac{1}{2\mu}\Delta_\Gamma)^{-1/2} \end{bmatrix}^{-1}. \tag{4}$$

We observe that the first two blocks form the classical Riesz map preconditioner for the Stokes subproblem, which can be easily discretized and for which efficient solvers are available. However, the Darcy pressure block is non-standard, combining the bulk Laplacian

[1] The pressure norm in the Stokes-Biot problem is analogous, see [1].

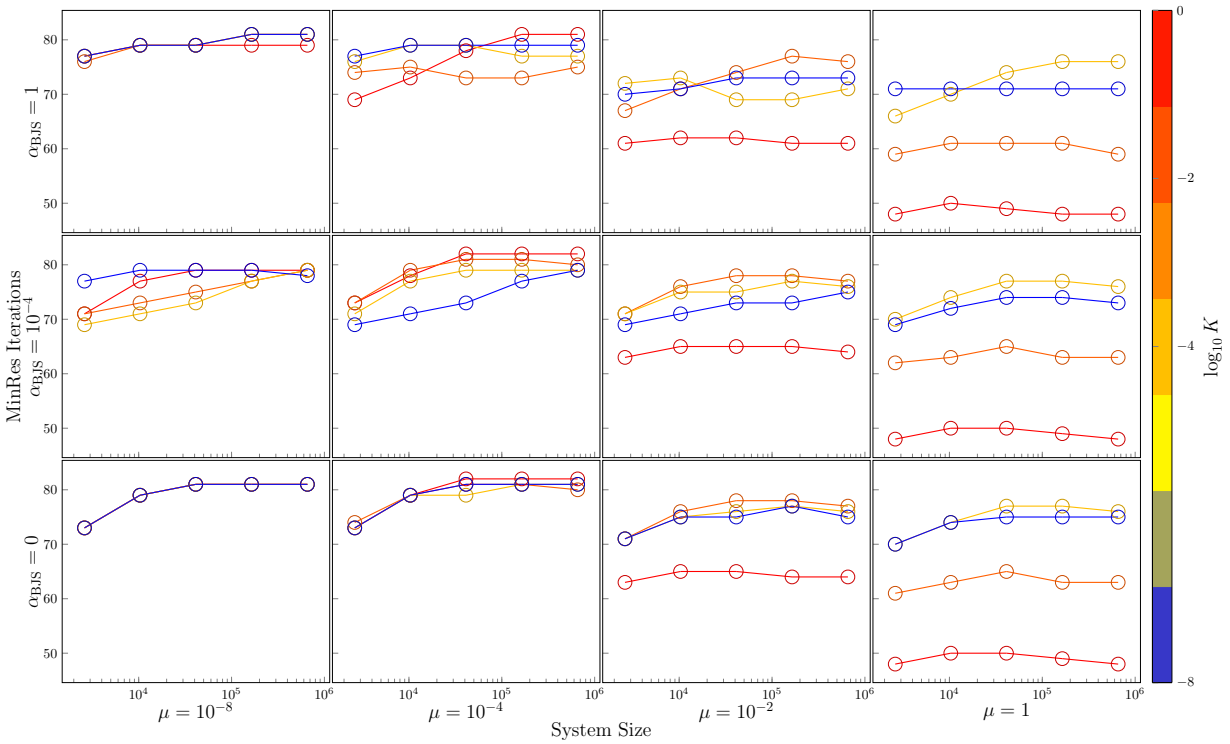

Figure 1: Number of preconditioned MinRes iterations for Stokes-Darcy problem with implicit coupling and different mesh resolution (increases along x-axis in each subplot) and values of Stokes viscosity μ (increases along main horizontal axis), Darcy permeability K (color encoded) and Beavers-Joseph-Saffman parameter (increases along main vertical axis). The system is discretized by lowest order Taylor-Hood elements for the Stokes subproblem and quadratic continuous Lagrange elements for the Darcy pressure. Fractional preconditioner (4) with blocks inverted by LU decomposition is used. Iterations are bounded in mesh size and the parameters.

(leading to a sparse matrix representation) with a dense block due to the fractional Laplacian. Scalable solvers for operators of this form, which are also robust in parameters (K, μ in (4)) are currently lacking.

To demonstrate robustness of (4) we utilize the definition of the fractional Laplacian based on spectral decomposition, assemble the exact matrix representation of the operator inducing the norm (3) and consider the exact realization of the preconditioner. In 1 we then finally present results of the sensitivity study for the Stokes-Darcy system [6]. It can be seen that the proposed fractional preconditioner yields iterations bounded in mesh size and the problem parameters.

References

[1] Wietse M Boon, Martin Hornkjøl, Miroslav Kuchta, Kent-Andre Mardal, and Ricardo Ruiz-Baier. Parameter-robust methods for the Biot-Stokes interfacial coupling without lagrange multipliers. *arXiv preprint arXiv:2111.05653*, 2021.

[2] Wietse M Boon, Timo Koch, Miroslav Kuchta, and Kent-Andre Mardal. Robust monolithic solvers for the Stokes-Darcy problem with the darcy equation in primal form. *arXiv preprint arXiv:2110.07486*, 2021.

[3] Boon, W. M. A parameter-robust iterative method for Stokes-Darcy problems retaining local mass conservation. *ESAIM: M2AN*, 54(6):2045–2067, 2020.

[4] Mingchao Cai, Mo Mu, and Jinchao Xu. Preconditioning techniques for a mixed Stokes/Darcy model in porous media applications. *Journal of computational and applied mathematics*, 233(2):346–355, 2009.

[5] Marco Discacciati and Luca Gerardo-Giorda. Optimized Schwarz methods for the Stokes–Darcy coupling. *IMA Journal of Numerical Analysis*, 38(4):1959–1983, 2018.

[6] Marco Discacciati, Edie Miglio, and Alfio Quarteroni. Mathematical and numerical models for coupling surface and groundwater flows. *Applied Numerical Mathematics*, 43(1-2):57–74, 2002.

[7] Juan Galvis and Marcus Sarkis. Balancing domain decomposition methods for mortar coupling Stokes-Darcy systems. In *Domain decomposition methods in science and engineering XVI*, pages 373–380. Springer, 2007.

[8] Karl Erik Holter, Miroslav Kuchta, and Kent-Andre Mardal. Robust preconditioning of monolithically coupled multiphysics problems. *arXiv preprint arXiv:2001.05527*, 2020.

[9] Qingguo Hong, Johannes Kraus, Maria Lymbery, and Fadi Philo. A new framework for the stability analysis of perturbed saddle-point problems and applications in poromechanics. *arXiv preprint arXiv:2103.09357*, 2021.

[10] M. Kuchta, M. Nordaas, J. Verschaeve, M. Mortensen, and K. Mardal. Preconditioners for saddle point systems with trace constraints coupling 2d and 1d domains. *SIAM Journal on Scientific Computing*, 38(6):B962–B987, 2016.

[11] Miroslav Kuchta and Kent-André Mardal. Iterative solvers for EMI models. In Aslak Tveito, Kent-Andre Mardal, and Marie E. Rognes, editors, *Modeling Excitable Tissue: The EMI Framework*, pages 70–86. Springer International Publishing, Cham, 2021.

[12] William J Layton, Friedhelm Schieweck, and Ivan Yotov. Coupling fluid flow with porous media flow. *SIAM Journal on Numerical Analysis*, 40(6):2195–2218, 2002.

[13] Kent-Andre Mardal and Ragnar Winther. Preconditioning discretizations of systems of partial differential equations. *Numerical Linear Algebra with Applications*, 18(1):1–40, 2011.

[14] M. Murphy, G. Golub, and A. Wathen. A note on preconditioning for indefinite linear systems. *SIAM J. Sci. Comput.*, 21:1969–1972, 2000.

Computational modelling of the interaction of hIFNγ C-terminal peptide and heparin-derived oligosaccharides

E. Lilkova[1], N. Ilieva[1,2], P. Petkov[3], L. Litov[3]
[1]Institute of Information and Communication Technologies, Bulgarian Academy of Sciences
[2]Institute of Mathematics and Informatics, Bulgarian Academy of Sciences
[3]Faculty of Physics, Sofia University "St. Kliment Ohridski"

Human interferon-gamma (hIFNγ) is a crucial immunomodulating cytokine, whose biological effects may range from proliferation to apoptosis. It mediates its pleiotropic action on cells by binding to the cell-surface domain of a high-affinity receptor hIFNγR1 to form a symmetric complex. On each side of the molecule there is a complex receptor-binding interface for each receptor that encompasses the N-terminal part of one monomer, and the C-terminal helix of the other monomer. The C-terminal domain of the cytokine does not appear to directly form a contact interface with the receptor. This part of the cytokine is a highly positively charged, solvent exposed tail, lacking a rigid conformation and is highly susceptible to proteolytic processing. The length of the C-tails plays a modulating role in the affinity of hIFNγ towards its receptor. In particular, the tetrapeptide Arg^{129}-Lys-Arg-Ser^{132}, greatly contributes to the high affinity interaction with hIFNγR1. Partial cleavage of the C-terminus (up to the 138 amino acid residue) does even lead to an increase in hIFNγ-hIFNγR1 binding affinity, whereas the removal of the complete tail causes inactivation of the cytokine.

IFNγ is known to bind to the glycosaminoglycans heparin and heparan sulfate (HS). These are linear negatively charged polymers of repeating disaccharide units, containing glucosamine and uronic acid, that can bear multiple N-sulfate, N-acetyl, and O-sulfate substitutions. The binding of hIFNγ to HS and heparin modulates the blood clearance, the subsequent tissue targeting, the local accumulation of the cytokine and the proteolytic processing of its C-terminal domain.

Here, we report molecular dynamics (MD) simulations studies of the interaction of a peptide, encompassing the last 21 C-terminal amino acid residues (AAKTGKRKRSQML-FRGRRASQ) of hIFNγ and a heparin-derived octasaccharide (dp8). The monosaccharide sequence of the carbohydrate was α-L-GlcA(1 $\rightarrow$ 4)β-D-GlcNS(6S)(1 $\rightarrow$ 4)α-L-

IdoA(2S)(1 → 4)β-D-GlcNS(6S)(1 → 4)α-L-IdoA(2S)(1 → 4)β-D-GlcNS(1 → 4)β-D-IdoA(1 → 4)β-D-GlcNAc and is presented schematically in Fig. 1.

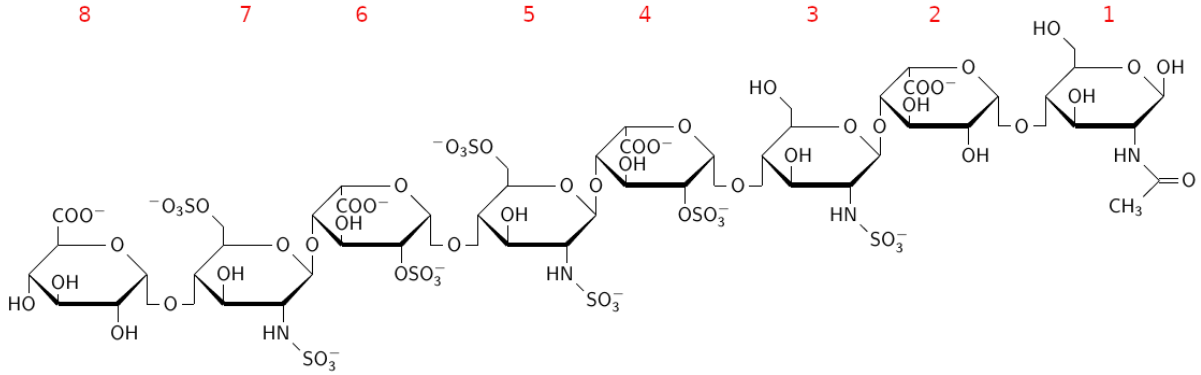

Figure 1: Octasaccharide sequence with monomer positions indicated in red.

The IFNγ C-terminal peptide was constructed in a completely extended conformation and was subjected to three independent folding simulations, amounting to a total of 1.5μs of simulation time. The dp8 structure was generated using the CHARMM-GUI server and was simulated for 100 ns. Cluster analysis was applied to identify the most visited conformations and the centroids of the five largest conformational clusters from both the hIFNγ C-terminal peptide and the octasaccharide were selected as input structures. Five independent 1μs simulations were performed, starting from randomly chosen input conformations and random mutual orientations of the two binding partners.

The interaction of the two molecules is dominated by strong electrostatic attraction, as the C-terminal peptide has a net charge of +8, and the dp8 has a net charge of -11. Binding of the two partners occurs almost immediately in the first few hundred picoseconds. Nonetheless, the binding residues differ due to the different initial orientations of the charged monosaccharides and peptide amino acid residues. To avoid possible initial-conditions bias, only the last 250ns of the five MD trajectories, combined into a single ensemble of conformations, were used to construct a contact map of the interaction of the peptide and the carbohydrate chains. The result is presented in Fig. 2.

The contact map reveals the existence of preferential positions for close contacts between the octasaccharide and the hIFNγ C-terminal peptide. With the exception of the first one, all carbohydrate monomers are negatively charged, the 4–7 segment having the highest negative charge density with a net negative charge of -2 for each monomer. As seen in Fig. 2, this part of the carbohydrate chain is responsible for the majority of the contacts with the peptide. On the other hand, the hIFNγ C-terminal peptide has two distinct basic domains – D1 (^{3}KTGKRKR^{9} with a +5 charge) and D2 (^{14}RGRR^{17}, carrying a +3 charge). Indeed, the highest contact occupancy is observed within these domains, but in particular at residues 3, 6–9, 14 and 17.

The computational approach advocated above appears to be both guiding and conclusive in scrutinizing the interaction of the C-terminal peptide of hIFNγ and heparin-derived

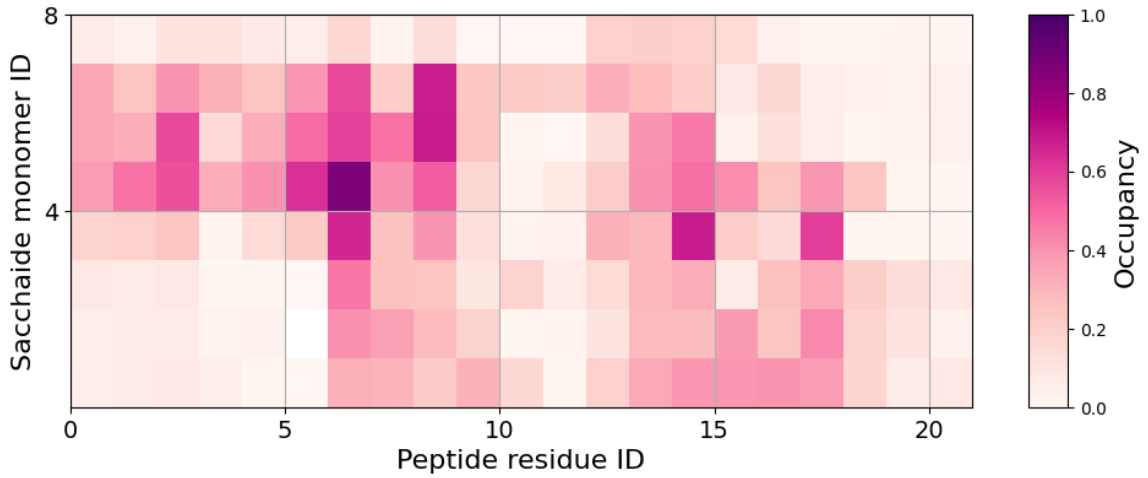

Figure 2: Contact map, averaged over the last 250 ns of the 5 independent simulations.

oligosaccharides for optimisation of the net charge and the positions of the sulfate groups of the carbohydrate chains in the process of drug design.

Acknowledgements This work was supported in part by the Bulgarian National Science Fund under Grant DN-11/20/2017. Computational resources were provided by the Centre for Advanced Computing and Data Processing, supported under Grant BG05M2OP001-1.001-0003 by the Science and Education for Smart Growth Operational Program (2014-2020) and co-financed by the European Union through the European structural and investment funds.

Numerical simulations and stability analysis for a fractional-order model on COVID-19

[1,2] Shaher Momani, [1,3] Iqbal M. Batiha
[1] Nonlinear Dynamics Research Center (NDRC), Ajman University Ajman 346, United Arab Emirates
[2] Dept. of Math., Fac. Sci., The University of Jordan, Amman 11942 Jordan
[3] Dept. of Math., Fac. Sci. and Techn., Irbid National University, 2600 Irbid, Jordan

Multiple nonlinear models for characterizing dynamics of COVID-19 outbreak have been recently established and discussed in literature. In view of such models, we endeavour in this work to detect the role of fractional calculus in addressing the COVID-19 dynamics turned more recently up in Jordan over 63 days; from 10 Dec 2021 to 10 Feb. 2022.

This mission will be accomplished by a mathematical model based on the Caputo fractional-order differential operator as opposed to the traditional integer-order one. One of SEIR models proposed recently will be employed to achieve this objective.

Numerical simulations will be carried out by implementing the Generalized Euler Method (GEM). For these purposes, the stability analysis of the presented fractional-order model will be examined in light of outlining its equilibrium points and identifying its reproduction number. Through performing some numerical comparisons, it will be proved that the results generated by using the fractional-order model is significantly closer to the aforesaid collected real data than that of the integer-order model. This would undoubtedly clarify the role of fractional calculus in facing epidemiological hazards.

Graph representation of the IgM antibody repertoire

A. Pashov[1], Sh. Pashova[2], P. Petrov[3]

[1]Institute of Microbiology, Bulgarian Academy of Sciences
[2]Institute of Biology and Immunology of Reproduction,
Bulgarian Academy of Sciences
[3]Institute of Mathematics and Informatics,
Bulgarian Academy of Sciences

Recently, the global analysis of the antibody repertoire has been used as a source of biomarkers for diverse processes involving immune and inflammatory activity [1, 2]. It is now part of the multiomics paradigm of systems biology. The repertoire studies develop in two directions – repertoire sequencing (RepSeq) and functional probing of the repertoire (igome) using arrays of diverse structures (e.g., peptides or glycans). The igome technique uses high throughput probing of the repertoire with a phage display random peptide library followed by next generation sequencing [3]. It yields 10^5–10^6 different sequences, each a target for at least one antibody in the repertoire. These peptide ligands approximate the nominal epitope for a given antibody, hence they are referred to as mimotopes.

Previously, sequence graphs were successfully used to extract system level biological information from repertoire sequencing data [4]. We applied a similar approach to integrate igome data. In both applications of graphs, a suitable metric for sequence similarity is used – Levenshtein distance in repertoire sequencing and longest common subsequence for the igome graph. Both systemic views of the repertoire yield small world type of networks evolving through random attachment (Fig. 1). This consistency of the network topology is intriguing because in the genetic signatures it is due to sequence evolution, while in the igome it is reflection of antibody cross-reactivity, hence – immunological co-selection. The two processes are ultimately related biologically and this is what the graph topology invariance reflects. In our first analysis, a graph of the IgM igomes in antiphospholipid syndrome showed existence of clusters of mimotopes reflecting mostly underexpressed and fewer overexpressed reactivities when compared to healthy controls. A key feature of the IgM igome proved to be mirroring sequences from the binding site (paratope) of other antibodies. Together these results of graph analysis are consistent with a disturbance creating a hole in the autoimmune IgM repertoire. Interestingly, a third view of the repertoire – probing it by a binding assay using a large array of peptides, yielded a graph of reactivities with the same topology as the repertoire sequencing graph and the igome graph. In this case each peptides IgM reactivity was tested in 21 patients and the resulting

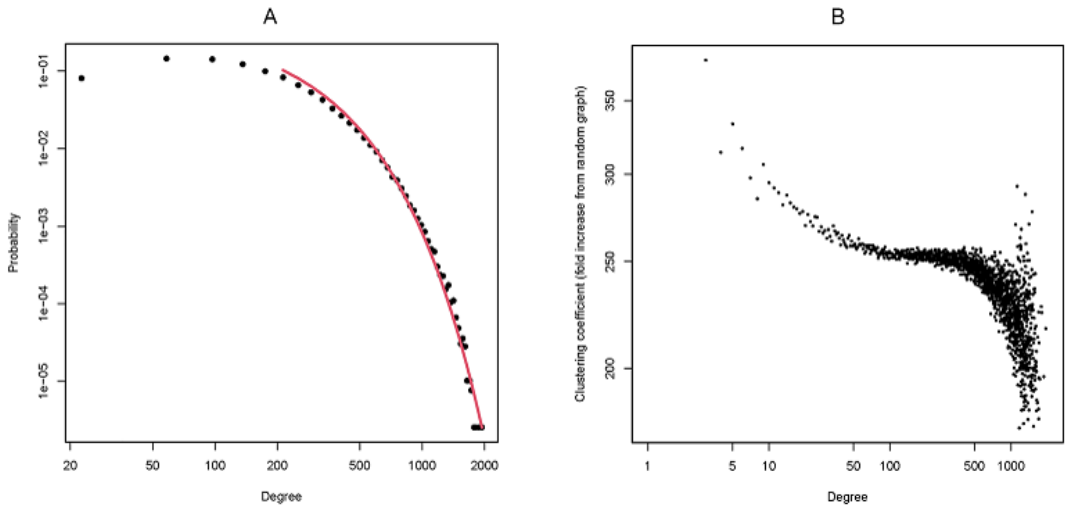

Figure 1: Degree distribution (A) and clustering coefficient dependence on degree (B) of the graph of mimotope sequences in the IgM igome. The degree distribution follows an exponential law while the local clustering coefficient is much higher than expected for a random graph and falls with the increase of the degree – both features of graphs with random attachment.

profiles were compared using F-test. Thus, the graph analysis of the antibody repertoire yields biologically interpretable characteristics which are found invariant of the technical approach to the repertoire study.

Acknowledgements This work was supported in part by the Bulgarian National Science Fund under Grant KP-06-COST-9/2019 "Topological aspects of biomolecular dynamics".

References

[1] S. Pashova, L. Balabanski, G. Elmadjian, A. Savov, E. Stoyanova, V. Shivarov, P. Petrov, and A. Pashov, Restriction of the Global IgM Repertoire in Antiphospholipid Syndrome. Front Immunol **13** (2022) 1–15.

[2] A. Pashov, V. Shivarov, M. Hadzhieva, V. Kostov, D. Ferdinandov, K.-M. Heintz, S. Pashova, M. Todorova, T. Vassilev, T. Kieber-Emmons, L.A. Meza-Zepeda, and E. Hovig, Diagnostic Profiling of the Human Public IgM Repert–14.

[3] Y. Weiss-Ottolenghi, and J.M. Gershoni, Profiling the IgOme: meeting the challenge. FEBS Lett **588** (2014) 318–25.

[4] E. Miho, R. Rokar, V. Greiff, and S.T. Reddy, Large-scale network analysis reveals the sequence space architecture of antibody repertoires. Nature Communications **10** (2019) 1321.

Orchestrated membrane penetrations as a means of studying peptide-membrane specific affinity

P. Petkov[1*], N. Ilieva[2,3], E. Lilkova[2], L. Litov[1]

[1] Faculty of Physics, Sofia University "St. Kl. Ohridski", Sofia, Bulgaria
[2] Institute of Information and Communication Technologies, Bulgarian Academy of Sciences, Sofia, Bulgaria
[3] Institute of Mathematics and Informatics, Bulgarian Academy of Sciences, Sofia, Bulgaria

Antimicrobial peptides (AMPs) are a diverse class of short proteins (typically between 6 and 80 amino acid residues long) that are a key element of the nonspecific innate immunity in most organisms, displaying a wide range of antimicrobial, antifungal, antivarial and even anticancer effects [1]. Lately, AMPs have attracted great research interest in the context of strategies to combat multi-drug resistant bacterial infections [2]. Although it is commonly believed that the cationic and amphiphilic nature of these small proteins is the key to their activity, there is still no clarity about all the traits that define a peptide as antimicrobial.

№	Sequence	Length [aa]	Net charge
1	VGCIHEGI	8	-1
2	KKDVGIGIGG	10	+1
3	RVIGNWIGLGL	11	+1
4	WHSEGNVGINA	11	-1
5	KVKDNQWRP	9	+2
6	PRGSGGRGGSHGGGGIPP	18	+2
7	VNVVGGGGGIVGGGIGGGGM	20	0
8	IIIDGFGGGIIVEHDPGS	18	-3
9	GVSIIIGGNHGIIQGIEI	18	-1
10	MPEGINPGGIIGGGACIGERP	21	-1

Table 1: Putative antimicrobial peptides, isolated from the lightest fraction of the mucus of garden snail *Helix aspersa*.

Here we present a novel synthetic approach based on enhanced-sampling molecular modelling for the study and categorization of the interaction of newly isolated peptides

*peicho@phys.uni-sofia.bg

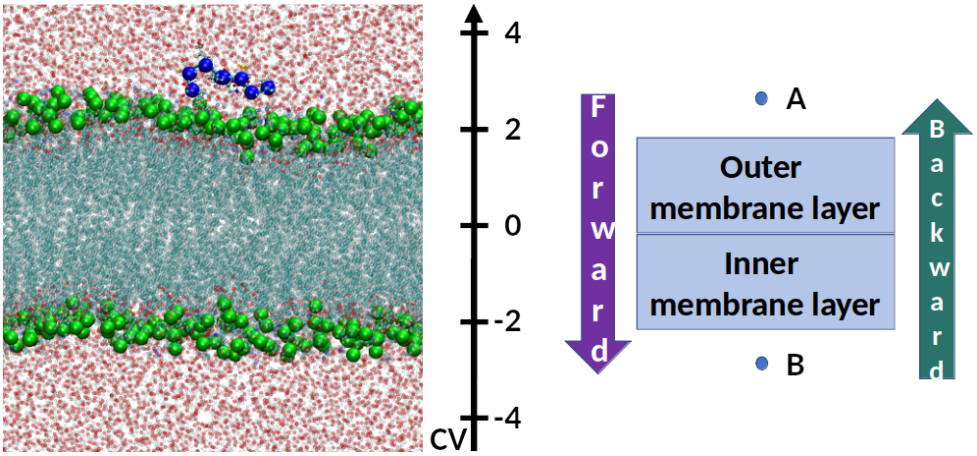

Figure 1: Metadynamics simulation input setup. The upper and lower membrane leaflets model the outer and inner bacterial membrane layers respectively.

(Table 1) from the lightest fraction (below 3 kDa) of the mucus of the garden snail *Helix aspersa*, known for its antimicrobial features [3, 4].

We propose that the free-energy profile of the process of peptide penetration and translocation within a model lipid bi-layer may shed light on the peptides' propensity to impact the bacterial membrane. To obtain this profile, metadynamics [5] was employed, with a biasing potential applied along a collective variable (CV) that describes the Z-projection of the distance between the center of masses (COMs) of the phospholipids' P atoms and the AMP C_α atoms. The simulation setup is depicted in Fig. 1. The P atoms were constrained along the Z-axis and movement allowed in the XY-plane only.

The model bacterial membrane was asymmetrically charged. The inner monolayer consisted of 70% POPE (neutral) and 30% POPG (negative) phospholipids and had twice as large charge density as the outer monolayer, containing 85 % POPE and 15 % POPG lipids. The CV thus constructed traversed an interval of 10 nm (from -5 nm to 5 nm) from the inner to the outer membrane leaflet. Two independent metadynamics simulations were performed for each peptide: a forward simulation, modeling the peptide translocation from the outer to the inner layer, and a backward simulation, modeling the process in the opposite direction (from the inner to the outer membrane layer). Based on the two simulations, the potential of mean force (PMF) along the selected CV was reconstructed and analyzed. For two of the peptides – peptide 3 and peptide 6 – no convergent simulations could be obtained within the above simulation setup, so these were discarded from further analysis. The obtained PMF profiles are presented in Fig. 2.

Our preliminary results reveal certain asymmetry in the free-energy barriers in the two leaflets of the membrane, promoting a directed translocation that cannot be associated with a single parameter. It is rather the charge distribution than the net charge that matters in this context, in combination with the specifics of the peptide amino acid content (the primary structure). Experimental validation of this hypothesis is ongoing.

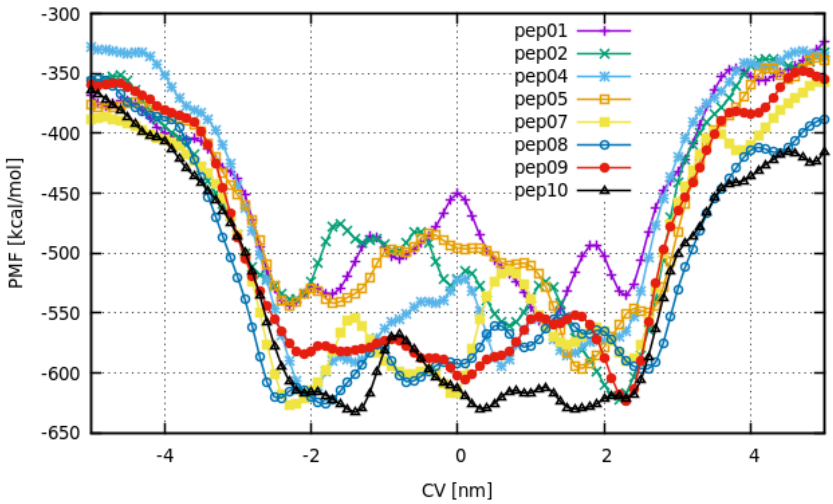

Figure 2: PMF profiles obtained from the converged simulations.

Acknowledgments This work was supported in part by the Bulgarian National Science Fund under Grant KP-06 OPR-03-10/2018. Computational resources were provided at the HPC cluster BioSim at the Faculty of Physics of Sofia University "St. Kl. Ohridski" and at CI TASK (Centre of Informatics – Tricity Academic Supercomputer & networK), Gdansk (Poland).

References

[1] Beutler, B. Innate immunity: an overview. Mol. Immunol. **40**(12) (2004) 845–859.

[2] López-Meza, J.E., Ochoa-Zarzosa, A., Barboza-Corona, J.E., Bideshi, D.K. Antimicrobial peptides: current and potential applications in biomedical therapies. BioMed Res. Int. Vol. 2015 (2015) 367243.

[3] Ilieva, N. et al. *In Silico* Study on the Structure of Novel Natural Bioactive Peptides. In: Lirkov I., Margenov S. (Eds) Large-Scale Scientific Computing. LSSC 2019. LNCS, **11958** (Springer, Cham, 2020) pp 332–339.

[4] Dolashki, A., Velkova, L., Daskalova, Zheleva, E., Topalova, Y., Atanasov, V., Voelter, W., and Dolashka, P. Antimicrobial Activities of Different Fractions from Mucus of the Garden Snail *Cornu aspersum*. Biomedicines **8**(9) (2020) 315.

[5] Laio, A., & Gervasio, F.L. Metadynamics: A method to simulate rare events and reconstruct the free energy in biophysics, chemistry and material science. Reports on Progress in Physics **71**(12) (2008) 126601.

Pohozhaev Identities and Applications to Nonlinear Mixed Type Equation

Nedyu Popivanov[1,3], Evgeny Moiseev[2], and Yani Boshev[3]

[1]Institute of Information and Communication Technologies, Bulgarian Academy of Sciences
[2]Lomonosov Moscow State University, Faculty of Computational Mathematics and Cybernetics
[3]Sofia University "St. Kliment Ohridsky", Faculty of Mathematics and Informatics

1 Introduction

Pohozhaev-type identities have been used in a large number of papers involving critical exponents, mostly related to elliptic problems. We can just mention here the seminal papers of Pohozhaev (1965), Serrin, Pucci (1986), Mitidieri, Pohozhaev (2003). In the critical case where the embedding fails to be compact the classical work of Brezis, Nirenberg (1983) must be mentioned.

Starting with the paper D. Lupo and K. Payne (2003), (2005) have also studied critical exponent phenomena for a class of mixed type elliptic-hyperbolic equations in multidimensional domains for the case of some classical boundary value problems. These ideas were further developed by Lupo, Payne, Popivanov (2005), establishing results for nonexistance of nontrivial regular solution both in two-dimensional case and in higher dimensions for Gellerstedt type operator in both supercritical and critical case.

An interesting topic is the application of Pohozhaev type identities in the study of nonexistence of nontrivial generalized solutions. Lupo, Payne and Popivanov (2014) studied the semilinear Goursat problem but in the frame of generalized solvability (instead of C^2 solutions) which is quite more natural for mixed type equations. They obtain nonexistence results for generalized solution in both supercritical and critical cases by applying the Pohozhaev type identity along a suitable regularized approximating sequence of smooth functions which approximate generalized solution. Extending these ideas to the semilinear Cauchy-Goursat problem Popivanov, Moiseev, Boshev (2018).

On the other hand, mixed-type problems with two degeneration lines in the linear case were studied by Nakhushev (1966), (1967), Zainulabidov (1969), Popivanov (1978) and many more.

For problems with two orthogonal degeneration lines containing nonlinearities, He, Liu [1] study

$$yu_{xx} + xu_{yy} = u|u|^{p-1} \quad in \quad B_r(0), \tag{1}$$

$$u = 0 \quad on \quad \partial B_r(0) \cup X \cup Y \cup AD, \tag{2}$$

where $B_r(0) \subset \mathbb{R}^2$ is a disc $\{|x| < r\}$, $X := B_r(0) \cap \{y = 0\}$, $Y := B_r(0) \cap \{x = 0\}$ and $AD := B_r(0) \cap \{x + y = 0\}$. They obtain result for nonexistence of nontrivial regular solution for the problem only in the critical case $p = 3$ by imposing Dirichlet boundary conditions on the external boundary but also on X and Y and on AD.

Remark 1. In our opinion such boundary value problems with some additional conditions on some segments inside the domain are strongly overdetermined and the statement of the problem in this case must be without these additional Dirichlet data.

2 Formulation of the problem

Find a solution of the differential equation

$$y|y|^{m-1}u_{xx} + x|x|^{m-1}u_{yy} + F'(u) = 0 \quad in \quad \Omega, \tag{3}$$

which satisfies the boundary condition

$$u = 0 \quad \text{on} \quad AB \cup BC \cup CD, \tag{4}$$

where $F'(u) = u|u|^{p-2}$, $p > 2$, $0 < m < 2$; $\Omega \subset \mathbb{R}^2$ is a mixed type domain consisting of two hyperbolic subdomains and an elliptic subdomain. The hyperbolic subdomains are bounded by characteristic lines OA, AB and OD, CD respectively and the elliptic arc is bounded by the arc BC. On the other characteristic lines (segments of the line $x + y = 0$), namely OA and OD where O is the origin, no boundary conditions are imposed. We obtain result for nonexistence of nontrivial regular solution for the problem (3), (4) by applying Pohozhaev type identity and the application of the exact Hardy-Sobolev inequality. The results are obtained for both supercritical case where $p > 2^*(2, m) = 4/m$ where $2^*(2, m)$ is the critical Sobolev exponent which arises from the embedding of the corresponding weighted Sobolev space $H^1_{0,m}(\Omega) \hookrightarrow L^p(\Omega)$ as well as for the critical case $p = 2^*(2, m)$.

3 Embedding theorems and critical exponents

Embeddings of type $H^1_0(\Omega) \hookrightarrow L^q(\Omega)$ have deep relationship with critical exponents phenomena. We distinguish supercritical case when the power of the nonlinearity is greater than Sobolev embedding constant, critical case when the power equals the constant and subcritical case which is when the power is less than the constant. A classical example is the one used in the seminal work of Pohozhaev (1965).

4 The Sobolev embedding theorem

Let Ω be a bounded smooth domain in $\mathbb{R}^n, n \in N$, $n \geq 3$. Then one has the embedding of $H_0^1(\Omega)$ into $L^q(\Omega)$ with $q \leq \dfrac{2n}{n-2}$. The critical Sobolev exponent is denoted by $2^*(n) := \dfrac{2n}{n-2}$ and the embedding is compact for $q \in [1, 2^*(n))$, but fails to be compact at the so called *critical case* when $q = 2^*(n)$.

There are certain weighted Sobolev spaces that are associated to equations of mixed type. Particular weighted Sobolev spaces associated to equation (3) will be with norm

$$||u||^2_{H^1_{0,m}(\Omega)} = \int_\Omega \left(|y|^m u_x^2 + |x|^m u_y^2\right) dxdy$$

where $\Omega \subset \mathbb{R}^2$, a bounded smooth domain and weights given by $(|y|^m, |x|^m)$.
Proposition 1: Let $m > 0$ be given. From the embedding $H^1_{0,m}(\mathbb{R}^2) \hookrightarrow L^q(\mathbb{R}^2)$ one obtains $q \leq 2^*(2, m) = \frac{4}{m}$.

5 Pohozhaev identity and nonexistence result

The Pohozhaev type identity for the problem (3) - (4) is given by

$$\int_\Omega \left(2 - \frac{m}{2}p\right) F(u)dxdy = \int_{AB\cup BC\cup CD} W_1 \cdot nds + \int_{OA\cup OD} (W_1 + W_2) \cdot nds, \qquad (5)$$

where the vector functions W_1 and W_2 are

$$W_1 = (xu_x + yu_y)(y|y|^{m-1}u_x, x|x|^{m-1}u_y) - \left(\frac{y|y|^{m-1}u_x^2 + x|x|^{m-1}u_y^2}{2}\right)(x, y),$$

$$W_2 = \frac{m}{2}u(y|y|^{m-1}u_x, x|x|^{m-1}u_y) + F(u)(x, y)\ .$$

and $F(u) := \int_0^u u|u|^{p-2}ds = \frac{|u|^p}{p}$ is the primary function of $F'(u)$ with $F(0) = 0$.

We must note the fact that boundary conditions are imposed on part of the boundary and there are parts where no information is given. Thus, in the respective Pohozhaev type identity there are additional boundary integrals whose sign must be evaluated. For that purpose key role plays Hardy-Sobolev inequality with remainder term.

$$\int_{-R}^0 (-t)^\alpha (w'(t))^2 dt \geq \frac{(\alpha-1)^2}{4} \int_{-R}^0 (-t)^{\alpha-2}(w(t))^2 dt + \frac{4}{R^2}\int_{-R}^0 (-t)^\alpha (w(t))^2 dt, \qquad (6)$$

with $w \in C^1(-R, 0) \cap C([-R, 0])$, $w(-R) = 0$ and $\alpha > 1$. This refinement of the classical Hardy-Sobolev inequality originates from the work of Brezis, Vasquez (1997) and is used for derivation of nonexistence results for critical growth phenomena for both regular and generalized solutions.

Theorem 1 *Let $\Omega \subset \mathbb{R}^2$ be a mixed type domain consisting of two hyperbolic subdomains and bounded elliptic subdomain. Let, $xn_x + yn_y \geq 0$ on the line BC in the elliptic part $\overline{\Omega}_3$. Let $u \in C^1(\overline{\Omega}) \cap C^2(\Omega)$ be a classical solution to (3) - (4) with $F'(u) = u|u|^{p-2}$. Then $u \equiv 0$ in the supercritical case $p > 2^*(2,m) = \frac{4}{m}$. If in addition on the elliptic arc BC the condition $xn_x + yn_y > 0$ holds, then the result $u \equiv 0$ holds also in the critical case $p = \frac{4}{m}$.*

Sketch of the proof: We are going to use (5) and by appropriate integration and rearrangement we will obtain contradiction for u being nontrivial. In addition, we will use also Hardy-Sobolev inequality (6) to ensure that the integrals over the segments OA, OD where no boundary conditions are imposed have appropriate sign.

Acknowledgments

The work of N. Popivanov and Y. Boshev was partially supported by Bulgarian NSF under Grant KP–06–Russia–126/2020.

References

[1] Ch. He, Ch. Liu, *Nonexistence for mixed-type equations with critical exponent nonlinearity in a ball*, Appl. Math. Lett. **24**, No. 5, 2011, 679-686.

[2] N. Popivanov, E. Moiseev, Y. Boshev, *Pohozhaev type identity for a nonlinear mixed type equation with two orthogonal degeneration lines*, AIP Conference Proceedings 2333, 120006 (2021); https://doi.org/10.1063/5.0041870.

Boundary value problems for fractional PDEs

Arsen V. Pskhu

Research Institute for Applied Mathematics and Automation,
Kabardino-Balkar Scientific Center, Russian Academy of Sciences,
Nalchik, Russia

Consider the equation

$$\left(\frac{\partial}{\partial x}+\frac{\partial^\alpha}{\partial y^\alpha}\right)u(x,y)=f(x,y)\qquad(0<\alpha<1),\tag{1}$$

where $\frac{\partial^\alpha}{\partial y^\alpha}$ is the Liouville fractional derivative of order α, which is defined as follows [1, § 2.3]

$$\frac{\partial^\alpha}{\partial y^\alpha}u(x,y)=\frac{\partial}{\partial t}\int_{-\infty}^{y}\frac{(y-t)^{-\alpha}}{\Gamma(1-\alpha)}\,u(x,t)\,dt.$$

Note that the equation (1) is an example of one of the simplest fractional partial differential equations. In the limiting case (for $\alpha=1$), this equation turns into the first-order hyperbolic equation

$$\left(\frac{\partial}{\partial x}+\frac{\partial}{\partial y}\right)u(x,y)=f(x,y).\tag{2}$$

This simplicity and clarity can be a good motivation for studying equations of the form (1), including for comparing the properties of integer order PDEs with their fractional counterparts. This may contribute to a better understanding of what the presence of fractional differentiation in the equation can bring.

We also note that equations of the form (1) arise when solving diffusion and diffusion-wave equations of fractional order by the factorization method [2], in particular, based on the equality

$$\left(\frac{\partial}{\partial x}+\frac{\partial^\alpha}{\partial y^\alpha}\right)\left(\frac{\partial}{\partial x}-\frac{\partial^\alpha}{\partial y^\alpha}\right)=-\left(\frac{\partial^{2\alpha}}{\partial y^{2\alpha}}-\frac{\partial^2}{\partial x^2}\right).$$

Moreover, such equations (1) appear in mathematical modeling of population dynamics (e.g., see [3]).

The study of fractional PDEs of order ≤ 1 began not so long ago, but nevertheless has a wide bibliography. Apparently, the first works devoted to such equations were the papers

[4] and [5] (see also [6]). Later, for such equations, as well as their generalizations, various initial and boundary value problems were considered, including problems in multidimensional domains and domains with curvilinear boundary, non-local problems, equations with variable and matrix coefficients, equations with fractional discrete-distributed differentiation operators, etc. A survey giving an idea of the main approaches can be found in [7].

Most of the papers dealt with fractional differentiation operators defined on a finite interval (having the origins at the finite points). In (1), we consider the Liouville fractional derivative, which has the origin at minus infinity.

Such equations induce asymptotic problems (problems without initial conditions). For these problems, instead of the initial conditions, it is necessary to specify the asymptotics of the desired solution. Here we consider just such a problem.

Let

$$\Omega = (r, a) \times (-\infty, b) = \{(x, y) : \, x \in (r, a), \, y \in (-\infty, b)\} \qquad (r < a)$$

and

$$\Omega_r = \Omega \cup \{(x, y) : \, x = r, y < b\}, \qquad \Omega^{\varepsilon} = (r, a - \varepsilon) \times (-\infty, b - \varepsilon).$$

A function $u(x, y)$ is called a *regular solution* of the equation (1) in the domain Ω if: $u(x, y) \in C(\Omega_r) \cap C_x^1(\Omega)$; $D_{-\infty y}^{\alpha-1} u(x, y) \in C_y^1(\Omega)$; $(R - y)^{-\alpha} u(x, y) \in L(-\infty, R)$ (as a function of y, $\forall x \in (r, a)$ and $R < b$); $u(x, y)$ satisfies the equation (1) in Ω.

We consider the following **problem**: *find a regular solution* $u(x, y)$ *of the equation* (1) *in the domain* Ω *satisfying the condition*

$$u(r, y) = \varphi(y) \qquad (y < b). \tag{3}$$

Define the function

$$w_{\mu}(x, y) = y^{\mu-1} \phi\left(-\alpha, \mu; \, -\frac{x}{y^{\alpha}}\right) \qquad (x, \, y > 0),$$

where

$$\phi\left(\xi, \eta; \, z\right) = \sum_{k=0}^{\infty} \frac{z^k}{k! \, \Gamma(\xi k + \eta)} \qquad (\xi > -1)$$

is the Wirght function [8], [9].

Now, we formulate the main results of the work.

Theorem 1 *Let* $f(x, y) \in L\left(\Omega^{\varepsilon}\right)$, $\varphi(y) \in L(-\infty, b - \varepsilon)$ *and*

$$\lim_{R \to -\infty} \sup_{\substack{x \in (r, a-\varepsilon) \\ y < R}} |u(x, y)| = 0, \tag{4}$$

for any sufficiently small $\varepsilon > 0$.

If $u(x,y)$ is a regular solution of the problem (1) *and* (3), *then*

$$u(x,y) = \int_{-\infty}^{y} \varphi(t)\, w_0(x-r, y-t)\, dt +$$

$$+ \int_{r}^{x} \int_{-\infty}^{y} f(s,t)\, w_0(x-s, y-t)\, dt\, ds. \tag{5}$$

The proof of Theorem 1 is based on a modification of the Green function method. An immediate consequence of Theorem 1 is the statement about the uniqueness of the solution of the problem under consideration.

Theorem 2 *There is at most one regular solution to the problem* (1) *and* (3) *in the class of functions satisfying* (4).

Note that Theorem 1 does not imply that any function of the form (5) is a priori a solution to the problem (1) and (3). In order this to be the case, it is necessary to impose additional conditions on the right side $f(x,y)$ and the boundary function $\varphi(y)$. The following statement gives such conditions.

Theorem 3 *Let* $\varphi(y) \in C(-\infty, b) \cap L(-\infty, b-\varepsilon)$, $f(x,y) \in C(\Omega_r) \cap L(\Omega^\varepsilon)$,

$$\lim_{y \to -\infty} (-y)^\delta \varphi(y) = 0 \qquad (\delta > 1 - \alpha),$$

and let $f(x,y)$ *be representable in the form*

$$f(x,y) = D_{rx}^{-\xi}\, D_{-\infty y}^{-\eta}\, g(x,y) \qquad (\xi > 0,\ \eta > 0),$$

where $g(x,y) \in L(\Omega^\varepsilon)$, $(x-r)^\mu g(x,y) \in C(\Omega_r)$ *and*

$$\sup\{(x-r)^\mu (b-y)^\nu |g(x,y)| :\ (x,y) \in \Omega^\varepsilon\} \le C, \qquad C = C(\varepsilon),$$

for some $\mu < \xi$, $\nu > \eta + 1$ *and for any suffucuently small* $\varepsilon > 0$.

Then the function $u(x,y)$ *defined by* (5) *is a regular solution to the problem* (1) *and* (3).

Theorem 3 is proved by a direct verification.

A notable consequence of the above statements is the fact that the solutions of the homogeneous equation (1) turn out to be analytic functions of the variable x for each fixed $y < b$. This property contrasts markedly with the case of equations with the Riemann-Liouville derivatives, which have the origins at finite points, and differs sharply from the case of equation (2).

References

[1] Kilbas A.A., Srivastava H.M., Trujillo J.J. *Theory and Applications of Fractional Differential Equations*; Elsevier: Amsterdam, The Netherlands, 2006; Volume 204.

[2] Pskhu A.V. Solution of the First Boundary Value Problem for a Fractional-Order Diffusion Equation. *Differential Equations,* 2003, **39**:8, 1359–1363. https://doi.org/10.1023/B:DIEQ.0000012703.45373.aa

[3] Losanova F.M., Kenetova R.O. Non-local problem for generalized McKendrick-von Foerster equation with Caputo operator. *Nonlinear World,* 2018, **16**:1, 49–53.

[4] Clément Ph., Gripenberg G., Londen S-O. Schauder estimates for equations with fractional derivatives. *Transactions of the American Mathematical Society,* 2000, **352**:5, 2239–2260.

[5] Pskhu A.V. Boundary Value Problem for a Differential Equation with Partial Derivatives of Fractional Order. *Reports of Adyghe (Circassian) International Academy of Sciences,* 2000, **5**:1, 45–53.

[6] Pskhu A.V. Solution of a Boundary Value Problem for a Fractional Partial Differential Equation. *Differential Equations,* 2003, **39**:9, 1150–1158. https://doi.org/10.1023/B:DIEQ.0000011289.79263.02

[7] Bogatyreva F.T. Boundary Value Froblems for a First Order Partial Differential Equation with the Dzhrbashyan–Nersesyan Operators. *Chelyabinsk Physical and Mathematical Journal,* 2021, **6**:4, 403–416.

[8] Wright E.M. On the coefficients of power series having exponential singularities. *J. London Math. Soc.* 1933, **8**, 71–79.

[9] Wright E.M. The generalized Bessel function of order greater than one. *Quart. J. Math. Oxford Ser.* 1940, **11**, 36–48.

On the application of HSS-compression for numerical solution of space-fractional parabolic problems: complexity and scalability

Dimitar Slavchev, Svetozar Margenov
Institute of Information and Communication Technologies
Bulgarian Academy of Sciences

1 Introduction

The fractional-in-space elliptic operators of power $\alpha \in (0,1)$ are utilized in modeling *anomalous* diffusion. Such models are used in image processing, financial mathematics,a electromagnetistics, peridynamics, flows in porous media, just to name a few.

Consider the parabolic equation $\partial u(x,t)/\partial t + (-\Delta)^\alpha u(x,t) = f(x,t)$, where $(-\Delta)^\alpha$ stands for the fractional Laplacian with homogeneous boundary conditions and initial condition $u^0(x)$. The problem is non-local and in general its numerical solution is very expensive. We are studying the application of Hierarchical Semi-Separable (HSS) compression for the efficient solution of discrete time-dependent fractional diffusion problems.

2 Fractional parabolic problem

Here, the *integral* definition of the fractional Laplace operator is assumed. The Finite Element Method (FEM) is employed for the approximation in space as outlined in [1], while the backwards Euler scheme, described in [3] is used for the discretization in time. In the case of *spectral* fractional Laplacian, a similar problem is examined in [4]. Unlike [4], in this article we provide an experimental comparative analysis for the case when the initial condition $u^0(x)$ is piece-wise constant, that is, the solution is less regular.

Applying the FEM discretization in space, we get the Cauchy problem

$$M_L \frac{d\mathbf{u}}{dt} + K\mathbf{u} = M_L\mathbf{f}, \quad 0 < t \le T, \quad \mathbf{u}(0) = \mathbf{u}^0,$$

for the unknown functions $\mathbf{u} = (u_j(t)) \in \mathbb{R}^n$, $t \in [0,T]$ and right hand side $\mathbf{f} = (f_j(t)) \in \mathbb{R}^n$. Here $K = K_{ij} \in \mathbb{R}^{n\times n}$ is the stiffness matrix corresponding to the *fractional* Laplacian. With $M_L = \mathrm{diag}\,(m_L^i) \in \mathbb{R}^n$ we denote the lumped mass matrix.

For the discretization in time we use the fully implicit backward Euler method with uniform time step τ

$$M_L \frac{\mathbf{u}^{j+1} - \mathbf{u}^j}{\tau} + K\mathbf{u}^{j+1} = M_L \frac{\mathbf{f}^{j+1} + \mathbf{f}^j}{2}, \quad j = 0, \ldots, m-1,$$

where m is the number of time steps,

$$m\tau = T, \quad t_0 = 0, \quad t_{j+1} = t_j + \tau \quad \text{and} \quad \mathbf{u}^j = \mathbf{u}(t_j), \quad \mathbf{f}^j = \mathbf{f}(t_j).$$

The following test problem is used in the presented numerical experiments: $(x,t) \in \Omega \times [0,T] = (-1,1)^2 \times (0,0.1)$, right hand side $f(x) = 0$, m time-steps, $\alpha = 0.5$, and initial condition defined by the checkerboard function

$$u^0(x) = \begin{cases} 1, & x \in [0,0.5]^2 \\ 0, & \text{otherwise.} \end{cases}$$

On Fig. 1 we present the initial condition u^0 and the solution in $t = 0.025$, 0.05, 0.075 and 0.1. The pictures illustrate the process of smoothing the initial data during the evolution.

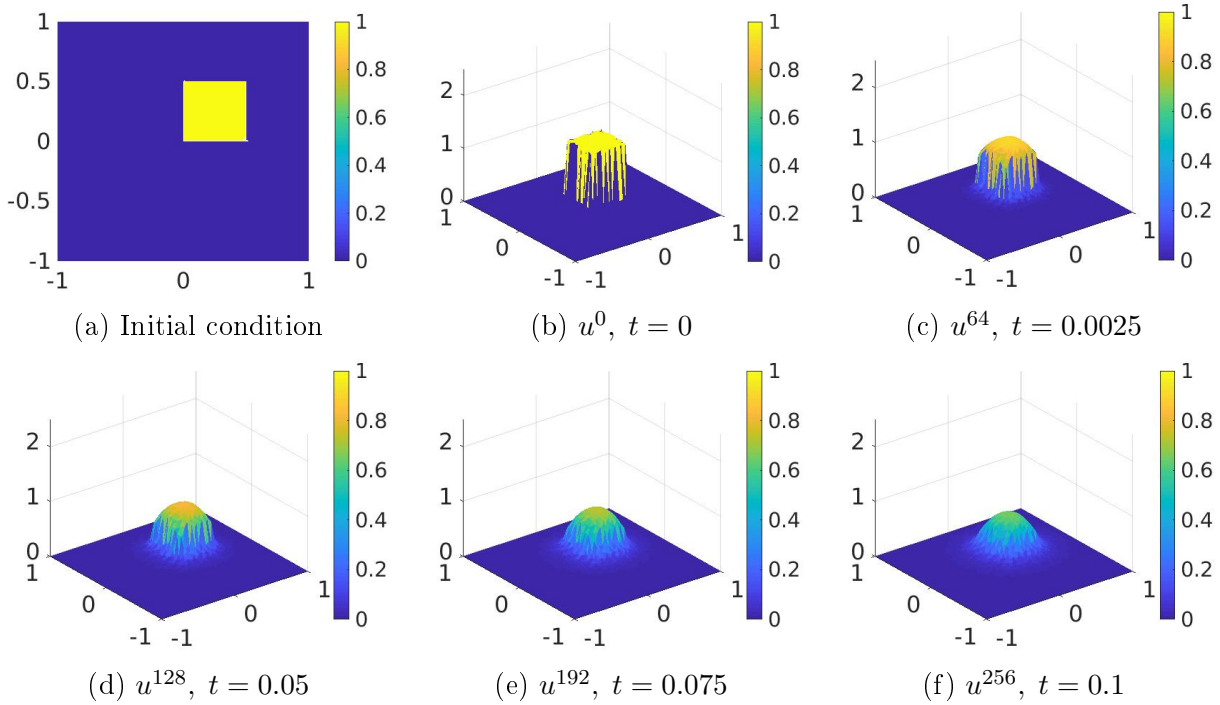

(a) Initial condition (b) u^0, $t = 0$ (c) u^{64}, $t = 0.0025$

(d) u^{128}, $t = 0.05$ (e) u^{192}, $t = 0.075$ (f) u^{256}, $t = 0.1$

Figure 1: Initial condition u^0 and solution at several time points.

3 Hierarchical Semi-Separable Compression

The Hierarchical Semi-Separable (HSS) compression belongs to the hierarchical group of methods for solving systems of linear algebraic equations. In a nutshell, these methods are used to *compress* the original coefficient matrix A into an hierarchical representation H. This form of the matrix takes less space and allows computations to be carried out more efficiently. The compression requires that the original matrix has proper *structure*, i.e. that the off-diagonal blocks of A have low rank. In this work we use the HSS solver implemented in the STRUctured Matrices PACKage (STRUMPACK) [2]. The algorithm works in three steps:

1. HSS compression. The original matrix is compressed into HSS form H. The computational complexity is $O(n^2 r)$, where n is the number of unknowns and r is the maximum rank of the off-diagonal blocks,

2. ULV-like factorization. The compressed form H of the matrix is then factorized in a modified form of ULV factorization. The computational complexity is $O(nr^2)$,

3. Solving the linear algebraic system with the factorized matrix. Uses the factorized matrix and the right hand side to obtain the solution. The computational complexity is $O(rn)$.

The overall computational complexity is $O(n^2 r)$, where $r \ll n$ for suitable problems. The goal is to compete with the computational complexity $O(n^3)$ of the Gaussian elimination solvers. As will be shown in the next section, the accuracy and efficiency of the HSS compression also depend on the relative ε_{rel} and absolute ε_{abs} thresholds specified by the user.

4 Comparative analysis

On Fig. 2 we present a comparison of the computational times obtained by the block LU factorization solver from the MKL package and the HSS compression based solver from STRUMPACK. We fix $\varepsilon_{abs} = 10^{-8}$ and vary $\varepsilon_{rel} \in \{10^{-2}, 10^{-4}, 10^{-6}, 10^{-8}\}$. The better computational complexity of the hierarchical method leads to better execution times both for the sequential and parallel tests.

On Fig. 3 we present the computational times of the different parts of the HSS based solver. We should note that the compression and factorization steps are executed only once, while solving systems with the factorized matrix is repeated at each time step. In this way, the solving steps have a greater impact on the total execution time than the computationally more expensive compression and factorization steps.

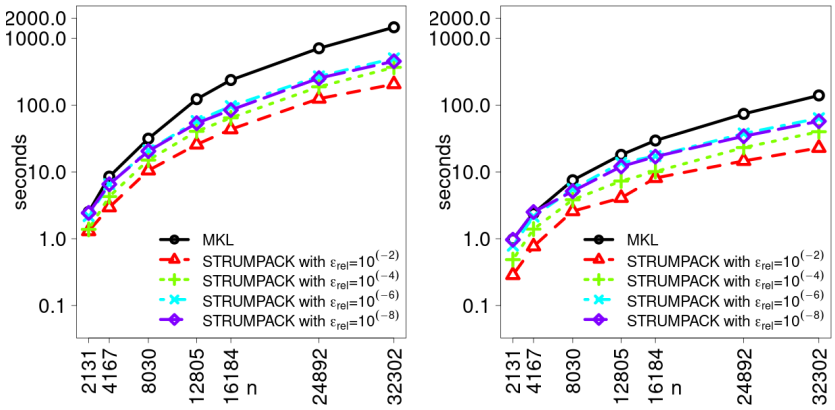

(a) Sequential (b) 16 threads

Figure 2: Comparison of MKL and HSS solvers.

5 Concluding remarks

In this work we analyze the performance of a hierarchical solver for a parabolic fractional diffusion problem. The HSS based solver compares favorably with the direct Gaussian solver from MKL in both the sequential and parallel experiments.

Acknowledgements

We acknowledge the provided access to the e-infrastructure and support by the Grant No BG05M2OP001-1.001-0003, financed by the Science and Education for Smart Growth Operational Program (2014-2020) and co-financed by the European Union through the European structural and Investment funds. The work has been partially supported by the Bulgarian National Science Fund under grant No. BNSF-DN12/1.

References

[1] Acosta, G., Borthagaray, J.P.: A Fractional Laplace Equation: Regularity of Solutions and Finite Element Approximations. *SIAM Journal on Numerical Analysis*, **55**, 472–495 (2017)

[2] Rebrova, E., Chávez, G., Liu, Y, Ghysels, P., Li, X.S.: A Study of Clustering Techniques and Hierarchical Matrix Formats for Kernel Ridge Regression. *2*018 IEEE International Parallel and Distributed Processing Symposium Workshops, 883–892 (2018)

[3] Slavchev, D., Margenov, S.: Performance Study of Hierarchical Semi-separable Compression solver for parabolic problems with spacefractional diffusion. Large-Scale Scientific Computing. *S*pringer Cham LNCS. **2019**, 71–80 (2022)

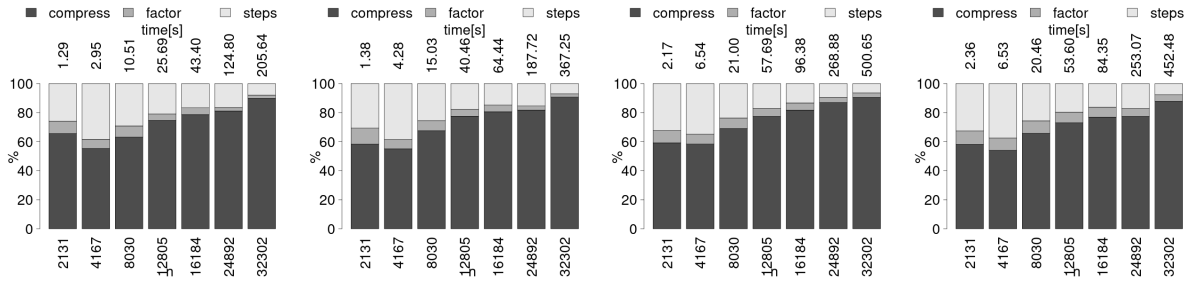

$\varepsilon_{rel} = 10^{-2}$ $\varepsilon_{rel} = 10^{-4}$ $\varepsilon_{rel} = 10^{-6}$ $\varepsilon_{rel} = 10^{-8}$

(a) Sequential results

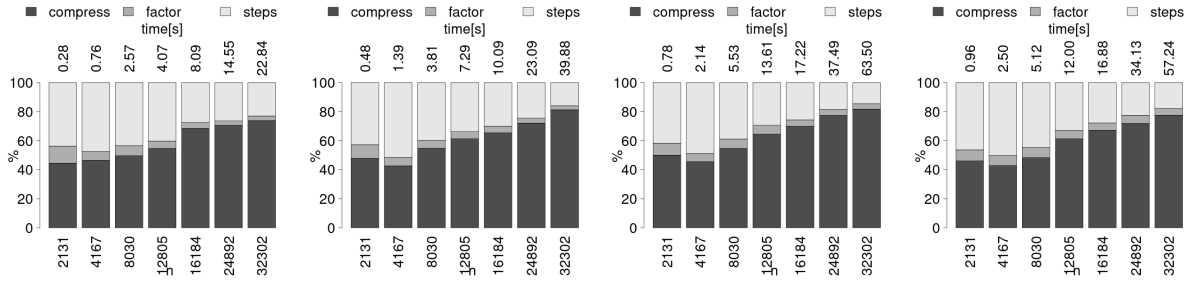

(b) $\varepsilon_{rel} = 10^{-2}$ (c) $\varepsilon_{rel} = 10^{-4}$ (d) $\varepsilon_{rel} = 10^{-6}$ (e) $\varepsilon_{rel} = 10^{-8}$

(a) 16 threads

Figure 3: Numerical results for $\alpha = 0.5$.

[4] Vabishchevich. P.: Splitting schemes for non-stationary problems with a rational approximation for fractional powers of the operator. *A*pplied Numerical Mathematics. **165**, 414–430 (2021)

Generalized finite difference method for a class of multidimensional space-fractional diffusion equations

HongGuang Sun[a,*], Zhaoyang Wang[a], Jiayi Nie[a], Yong Zhang[b], Rui Xiao[c]

a. State Key Laboratory of Hydrology-Water Resources and Hydraulic Engineering, College of Mechanics and Materials Hohai University, Nanjing, Jiangsu 210098, China.

b. Department of Geological Sciences, University of Alabama Tuscaloosa, AL 35487, United States

c. Key Laboratory of Soft Machines and Smart Devices of Zhejiang Province, Department of Engineering Mechanics Zhejiang University, Hangzhou 310027, China.

∗ Corresponding author: HongGuang Sun (shg@hhu.edu.cn)

Fractional diffusion equations have been widely used to accurately describe anomalous solute transport in complex media. This paper proposes a local meshless method named the generalized finite difference method (GFDM), to solve a class of multidimensional space fractional diffusion equations (SFDEs) in a finite domain. In the GFDM, the spatial derivative terms are expressed as linear combinations of neighboring-node values with different weighting coefficients using the moving least-square approximation. An explicit formula for the SFDE is then obtained. The numerical solution is achieved by solving a sparse linear system. Four numerical examples are provided to verify the effectiveness of the proposed method. Numerical analysis indicates that the relative errors of prediction results are stable and less than 1% ($0.001\% - 1\%$). The method can also be applied for irregular grids with acceptable accuracy.

Multiple solutions for a fractional discrete p-Laplacian boundary value problem

Stepan A. Tersian,
Institute of Mathematics and Informatics, Bulgarian Academy of Sciences,
Acad. G. Bonchev str. 8. Sofia 1113, Bulgaria

In this paper, we study the existence of at least three solutions for a fractional discrete boundary value problem

$$\begin{cases} {}_{T+1}\nabla_k^{\alpha}({}_k\nabla_0^{\alpha}(u(k))) +_k \nabla_0^{\alpha}({}_{T+1}\nabla_k^{\alpha}(u(k))) + \varphi_p(u(k)) = \lambda f(k, u(k)), \\ u(0) = u(T+1) = 0 \end{cases} \tag{1}$$

where $0 < \alpha < 1$, $\lambda > 0$, ${}_k\nabla_0^{\alpha}$ is the left nabla discrete fractional difference and ${}_{T+1}\nabla_k^{\alpha}$ is the right nabla discrete fractionl difference, $f : [1, T]_{\mathbb{N}_0} \times \mathbb{R} \to \mathbb{R}$ is a continuous function, φ_p is tho so called p-Laplacian operator defined as $\varphi_p(s) = |s|^{p-2}s$ and $1 < p < \infty$.

Several sufficient conditions for the existence of multiple solutions of the boundary value problem (1) are given. Our approach is based on the variational method. An example is presented to illustrate the applicability of the results.

Computational modeling of the replicase-transcriptase complex of SARS-CoV-2

N. Todorova[1], M. Rangelov[2], P. Petkov[3], N. Ilieva[4], E. Lilkova[4], and L. Litov[3]

[1] Institute of Biodiversity and Ecosystem Research, Bulgarian Academy of Sciences
[2] Institute of Organic Chemistry with Centre of Phytochemistry, Bulgarian Academy of Sciences
[3] Faculty of Physics, Sofia University "St. Kl. Ohridski"
[4] Institute of Information and Communication Technologies, Bulgarian Academy of Sciences

COVID-19 pandemic poses unprecedented societal challenges on a global scale with enormous medical, economic, political and ethical impact. To devise therapeutic strategies to counteract SARS-CoV-2 infection it is crucial to develop a comprehensive understanding of how the virus hijacks the host and inactivates its immune response during the course of the infection. This knowledge is indispensable for developing new drugs, alongside with repurposing existing ones.

To ensure its replication, the SARS-CoV-2 virus blocks the innate immune response of the host cell by interrupting mRNA transportation from nuclei to the cytoplasm and influences the IFN signalling pathway by preventing the transportation of STAT1 trough the nuclear pores thus blocking the expression of type I IFN induced genes. It was hypothesised that the SARS-CoV-2 Nsp13 protein influences the IFN type I production by interacting with two key players of IFN signalling pathway – TANK-binding kinase 1 (TBK1) and TANK-binding kinase 1-binding protein 1 (TBKBP1/SINTBAD [1]. We aim at ellucadating the mechanism of this interaction in order to unblock the inhibited interferon pathways. For this, we focused on the viral replicase-transcriptase complex (RTC), part of which is the helicase Nsp13.

We developed a precise model of the replicase-transcriptase complex of SARS-CoV-2 from the crystallographic structure deposited in Protein Data Bank (PDB ID 6XEZ [2]), adding the missing amino acids and nucleotides. Bigger missing parts were modeled *de novo* and the final structure of the complex was protonated by simulated physiological conditions of pH=7, T=300K, and salt content 0.15 M/l. A topology was created for the resultant structure with the software package GROMACS [3], accounting for Zn^{2+}

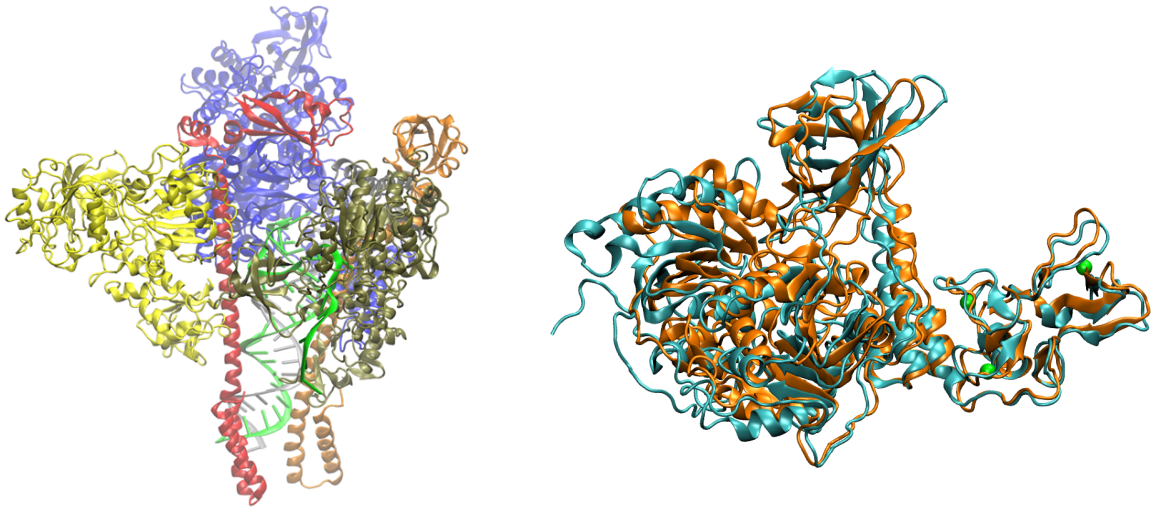

Figure 1: The replicase-transcriptase complex of SARS-CoV-2; PDB ID 6XEZ, Nsp8 in red, Nsp13 in yellow (left panel; Nsp13: PDB apo form in yellow, the structure after 330 ns of MD simulation, with parameterized Zn^{2+} ions in blue (right panel).

containing fragments of protein structure (Fig. 1). The contact sites between Nsp8 [4] and Nsp13 were identified and ranked based on their importance.

Further, similarities between Nsp8 and TBK1 were explored on the sequence level and with the secondary structure taken into account. To this end, all possible fragments derived from the Nsp8 sequence and longer than 10 amino acids were examined for similarities with all possible positions with respect to the TBK1 sequence [5] means of similarity matrices BLOSUM45, BLOSUM62, BLOSUM80 and BLOSUM90 [6, 7, 8]. The identified fragments with the highest degree of similarity were used for the assessment of the possibility of stable complexes formation between Nsp13 and TBK1.

Acknowledgements This work was supported in part by the Bulgarian National Science Fund under Grant KP-06-DK1/5/2021. Computational resources were provided at the HPC cluster BIOSIM at the Faculty of Physics of Sofia University "St. Kl. Ohridski".

References

[1] Gordon, D. et al. (2020) A SARS-CoV-2-Human Protein-Protein Interaction Map Reveals Drug Targets and Potential Drug-Repurposing. Nature **583** (2020) 459–468 doi

[2] Chen, J., Malone, B., Llewellyn, E., Grasso, M., Shelton, P.M.M., Olinares, P.D.B., Maruthi, K., Eng, E.T., Vatandaslar, H., Chait, B.T., Kapoor, T.M., Darst, S.A.,

Campbell, E.A. Structural Basis for Helicase-Polymerase Coupling in the SARS-CoV-2 Replication-Transcription Complex. Cell **182**(6) (2020) 1560–1573.e13 doi

[3] Abraham, M.J., Murtola, T., Schulz, R., Pll, S., Smith, J., Hess, B., Lindahl, E. GROMACS: High performance molecular simulations through multi-level parallelism from laptops to supercomputers. SoftwareX **1-2** (2015) 19–25.

[4] Wilamowski, M., Hammel, M., Leite, W., Zhang, Q., Kim, Y., Weiss, K.L., Jedrzejczak, R., Rosenberg, D.J., Fan, Y., Wower, J., Bierma, J.C., Sarker, A.H., Tsutakawa, S.E., Pingali, S.V., O'Neill, H.M., Joachimiak, A., Hura, G.L. Transient and stabilized complexes of Nsp7, Nsp8, and Nsp12 in SARS-CoV-2 replication. Biophys J. **120**(15) (2021) 3152–3165 doi

[5] Larabi, A., Devos, J.M., Ng, S.L., Nanao, M.H., Round, A., Maniatis, T., Panne, D. Crystal structure and mechanism of activation of TANK-binding kinase 1. Cell Rep. **3**(3) (2013) 734–746 doi

[6] Styczynski, M.P., Jensen, K.L., Rigoutsos, I., Stephanopoulos, G. BLOSUM62 miscalculations improve search performance. Nature Biotechnol. **26**(3) (2008) 274–275 doi

[7] Jianzhu Ma, Sheng Wan. Algorithms, Applications, and Challenges of Protein Structure Alignment. In: Rossen Donev (Ed). Advances in Protein Chemistry and Structural Biology, Vol. 94 (Academic Press, 2014), pp 121–175; ISSN 1876-1623, ISBN 9780128001684.

[8] Gauthier, J., Vincent, A.T., Charette, S.J., Derome, N. A brief history of bioinformatics, Briefings in Bioinformatics **20**(6) (2019) 1981–1996 URL

Exponent Splitting Schemes for Evolution Equations with Fractional Powers of Operators

Petr N. Vabishchevich
Nuclear Safety Institute, Russian Academy of Sciences, Moscow, Russia

We have considered the Cauchy problem for a first-order evolutionary equation with fractional powers of the operator. Such nonlocal mathematical models are used, for example, to describe anomalous diffusion processes. We want the transition to a new level in time to be solved common problems. Computational algorithms are constructed based on some approximations of operator functions. Currently, when solving stationary problems with fractional powers of the operator, the most attention is paid to rational approximations [1]. In the approximate solution of nonstationary problems, we come to equations with an additive representation of the problem operator [2]. Additive-operator schemes are constructed by using different variants of splitting schemes. In the present work, the time approximations are based on approximations of the transition operator by the product of exponents. We use exponent splitting schemes of the first and second-order of accuracy. The results of numerical experiments for a two-dimensional model problem with fractional powers of the elliptic operator are presented. **1. Problem formulation**. The object of our study is the Cauchy problem

$$\frac{du}{dt} + A^\alpha u = f(t), \quad 0 < t \le T, \tag{1}$$

$$u(0) = u^0. \tag{2}$$

The operator A is a self-adjoint positive definite operator in the finite-dimensional Hilbert space H. For the solution of the problem (1), (2), we have the representation

$$u(t) = \exp(-tA^\alpha)u^0 + \int_0^t \exp(-(t-s)A^\alpha) f(s) ds, \quad 0 < t \le T. \tag{3}$$

We approximate in time using a uniform grid with a step τ. We use the notation $y^n = y(t^n),\ t^n = n\tau,\ n = 0, \dots, N,\ N\tau = T$. From (3), we obtain

$$u^{n+1} = \exp(-\tau A^\alpha)u^n + \int_{t^n}^{t^{n+1}} \exp(-(t^{n+1}-s)A^\alpha) f(s) ds, \quad n = 0, \dots, N-1.$$

We consider an approach to an approximate solution of the problem (1), (2) with a prior approximation of A^α by some operator D. In this case we have

$$y^{n+1} = S(D)y^n + F^n(D, f), \quad n = 0, \dots, N-1, \tag{4}$$

where

$$D \approx A^\alpha,\ S(D) \approx \exp(-\tau D),\ F^n(A^\alpha, f) \approx \int_{t^n}^{t^{n+1}} \exp(-(t^{n+1}-s)A^\alpha) f(s) ds.$$

After choosing the operator D, we construct some approximations $S(D)$.

2. Rational approximation of the fractional power. For $A^\alpha,\ 0 < \alpha < 1$, we put

$$A^\alpha = AA^{-\beta}, \quad \beta = 1 - \alpha.$$

We use a rational approximation of A^α in the form

$$D = D(A) \approx A^\alpha, \quad D(A) = AR(A), \quad R(A) = a_0 I + \sum_{i=1}^{m} a_i (b_i I + A)^{-1} \tag{5}$$

with the coefficients

$$a_0 \geq 0, \quad a_i > 0, \quad b_i > 0, \quad i = 0, 1, \ldots, m.$$

The simplest approach to constructing a rational approximation of the operator $A^{-\beta}$ involves applying some quadrature formula for the integral on the right-hand side Balakrishnan formula

$$A^{-\beta} = \frac{\sin(\beta\pi)}{\pi} \int_0^\infty \theta^{-\beta} (\theta I + A)^{-1} d\theta, \quad 0 < \beta < 1.$$

In this work the best rational approximation was performed using the open-source Python package baryrat (https://github.com/c-f-h/baryrat).

3. Exponent splitting schemes. With a rational approximation (5) for the operator D, we have an additive representation

$$D = \sum_{i=0}^{m} D_i, \quad D_0 = a_0 A, \quad D_i = a_i A (b_i I + A)^{-1}, \quad i = 1, 2, \ldots, m. \tag{6}$$

For the operator terms in (6), we have

$$D_i = D_i^* \geq 0, \quad D_i D_j = D_j D_i, \quad i, j = 0, 1, \ldots, m. \tag{7}$$

Under the conditions (6), (7), we have

$$\exp(-\tau D) = \exp\Big(-\tau \sum_{i=0}^{m} D_i\Big) = \prod_{i=0}^{m} \exp(-\tau D_i). \tag{8}$$

Thereby the time transition operator from one level to another (the operator exponent $\exp(-\tau D)$) is split into the product of the operator exponents $\exp(-\tau D_i),\ i = 0, 1, \ldots, m$. Given (8), we can construct exponent splitting schemes when

$$S(D) = \prod_{i=0}^{m} S(D_i).$$

For the transition operator we use the representation

$$\exp(-\tau D) = S(D) + \tau^{\gamma} Q(D) + \mathcal{O}(\tau^{\gamma+1}).$$

In modern computational practice, the schemes of the first ($\gamma = 2$) and second ($\gamma = 3$) order of accuracy receive the most attention. When choosing a method for approximate solution of the Cauchy problem for a first-order evolution equation with a self-adjoint operator, instead of the standard unconditional stability condition, one can focus on the more stringent SM-stability conditions (Spectral Mimetic stability). In this case the scheme has ϱ-stability, spectral monotonicity and the scheme is asymptotically stable.

We construct unconditionally stable exponent splitting schemes using various approximations of the transition operator with account of pairwise permutation of operators $D_i(A),\ i = 0, 1, \ldots, m$. An implicit scheme of the first order of accuracy (analog of the implicit Euler scheme) and a symmetric scheme of the second order of accuracy (analog of the Crank-Nicholson scheme) are distinguished. SM-stable schemes to which the implicit Euler scheme belongs, but the Crank-Nicholson scheme does not belong, are of particular importance for computational practice. We have investigated two types of such exponent splitting schemes of second order accuracy.

The accuracy of the constructed exponent splitting schemes is illustrated by examples of calculations for a test two-dimensional problem with a fractional power of the Laplace operator using finite-difference approximations on a uniform grid over space. We investigated the influence of the power (α parameter) and the time step when using different exponent splitting schemes.

References

[1] S. Harizanov, R. Lazarov, and S. Margenov, A survey on numerical methods for spectral space-fractional diffusion problems, Fractional Calculus and Applied Analysis, 23 (2021), pp. 1605–1646.

[2] P. N. Vabishchevich, Splitting schemes for non-stationary problems with a rational approximation for fractional powers of the operator, Applied Numerical Mathematics, 165 (2021), pp. 414–430.

Enthalpy Solution of a Two-dimensional Fractional Stefan Problem

Vaughan R. Voller,
Civil, Environmental, and Geo- Engineering,
University of Minnesota,
Minneapolis, Minnesota, USA.

Here our interest is in the numerical solution of a Stefan melting problem [1] in a square domain $L \times L$. Initially the domain, insulated on all sides, is solid at the melting phase change temperature, $u = 0$. Melting is induced by setting the the boundaries along $x = 0$ and $y = 0$ to the fixed temperature $u = 1$. We write the governing equation for determining the evolution of the temperature field and the advance of the melting through time t in the domain as,

$$\frac{\partial^\alpha H}{\partial t^\alpha} = \frac{\partial^2 u}{\partial x^2} + \frac{\partial^2 u}{\partial y^2}, \quad 0 < \alpha \leq 1 \tag{1}$$

where, assuming a unit latent heat $l = 1$, the enthalpy is defined as

$$H(x, y, t) = \begin{cases} u(x, y, t) + 1, & \text{if } u(x, y, t) > 0 \\ 0, & \text{if } u(x, y, t) = 0 \end{cases} \tag{2}$$

As written the left hand side of the governing equation is expressed in terms of a RiemannâĂŞLiouville time fractional derivative of order $0 < \alpha \leq 1$. A setting of $\alpha = 1$ recovers the well known enthalpy model [1], where we should expect the standard diffusion scaling between length and time $\ell \sim t^{\frac{1}{2}}$. Due to the convenience of a single domain treatment, removing the necessity to explicitly track the melting front, the enthalpy formulation has been extensively used to model industrial melting problems, e.g., metal processing. In the cases where $\alpha < 1$ the given enthalpy formulation will apply to cases where the domain contains a distribution of heterogeneous length scales that disrupt the square root of time scaling, leading to anomalous transport where $\ell \sim t^{\frac{\alpha}{2}}$ [7].

In terms of one-dimensional problem domains, there have been a number of previous studies that have looked at Stefan problem formulations with fractional time derivatives [2, 3, 4, 5, 6]. These works have introduced numerical and analytical solutions, all of which clearly exhibit the expected anomalous transport scaling $\ell \sim t^{\frac{\alpha}{2}}$. In this work we have two objectives: (i) Extent the one-dimensional enthalpy solution introduced in [4] to two-dimensions. (ii) See if we can find a clear anomalous signal in the 2-D domain that recovers the scaling $\ell \sim t^{\frac{\alpha}{2}}$.

Following [4], we seek a time explicit, finite difference control volume solution of the governing enthalpy equation [eq.(1)]. The domain $L \times L$ is covered with a mesh of node centered square cells (size $\Delta \times \Delta$, $\Delta = \frac{L}{m}$) indexed by rows $i = 1, 2 \ldots, m$, and columns $j = 1, 2 \ldots, m$. This allows us to approximate the right hand side of eq.(1), as

$$\frac{\partial^2 u}{\partial x^2} + \frac{\partial^2 u}{\partial y^2} \approx \frac{u_{i-1,j} + u_{i+1,j} + u_{i,j-1} + u_{i,j+1} - 4u_{i,j} - u_l - u_b}{\Delta^2} \tag{3}$$

where at most nodes $u_l = u_b = 0$, but, to account for boundary conditions, the following settings are made, when $i = 1, u_{i-1,j} = 2, u_b = u_{i,j}$, when $i = n, u_{i+1,j} = 0, u_b = -u_{i,j}$, when $j = 1, u_{j-1,j} = 2, u_l = u_{i,j}$, and when $j = n, u_{i,j+1} = 0, u_l = -u_{i,j}$. We approximate the RiemannâĂŞLiouville time fractional derivative of the left of eq.(1) with the Grünwald weights, writing at time $t = k\Delta t$,

$$\frac{\partial^\alpha H_{i,j}^k}{\partial t^\alpha} \approx \frac{1}{\Delta t^\alpha} \sum_{p=0}^{k} g_p H_{i,j}^{j-p}, \tag{4}$$

where $g_p,\ p = 0, 1, \ldots,$ are the Grünwald weights

$$g_0 = 1, \quad g_p = g_{p-1} \left[\frac{p - 1 - \beta)}{p} \right],\ p = 1 \ldots k. \tag{5}$$

From eqs. (3) and (4) we propose the following time updating solution. The solution is initiated by setting $u_{i,j}^0 = H_{i,j}^0 = 0$. At time level $k > 0$ we solve the explicit equation

$$H_{i,j}^k = \frac{\Delta t^\alpha}{\Delta^2} \left(u_{i-1,j} + u_{i+1,j} + u_{i,j-1} + u_{i,j+1} - 4u_{i,j} - u_l - u_b \right) - \sum_{p=1}^{k} g_p H_{i,j}^{j-p} \tag{6}$$

at each node. From the time updated nodal enthalpy field, we use the relationship in eq.(2) to update the nodal temperature and liquid fraction fields,

$$u_{i,j}^k = \max(H_{i,j}^k - 1, 0), \quad f_{i,j}^k = \min(H_{i,j}^k, 1), \tag{7}$$

where the liquid fraction, constrained by $0 \le f_{i,j} \le 1$, can be used to track the progress of the melting phase change. Following this step, the calculations and updates for time level $k + 1$ can proceed.

We carry out the solution on a domain of size $(L =)30 \times 30$ with a space step $\Delta = 1$ and a time step $\Delta t = 0.1$. To quantify the behavior of the melting, we plot, with time, the position $(0 \le x \le L)$ of the melt front along the line $y = L = 30$. We denote this position as $s(t)$ and only record values when the melting, in a given control volume i completes the phase change, that is, as $f_i = 0$, we record the time t and set $s(t) = i\Delta x$. We find, across a range of values of α $[1.9, 0.9, 0.8, 0.7]$ that the predicted front position is almost perfectly fit by the power-law $s(t) = at^n$. The values of the exponents for given values of α are given in Table 1. We first note that, when $\alpha = 1$, the fit exponent is $n = 0.5025$, indicating,

Table 1: Exponnets of power-law fits $s = at^n$.

$\alpha = 1.0$	$\alpha = 0.9$	$\alpha = 0.8$	$\alpha = 0.7$
$n = 0.5025$	$n = 0.4504$	$n = 0.3980$	$n = 0.3530$

as expected a normal transport behavior. However, for other choices of the value α, the exponent is anomalous, recovering the values $n =\approx \alpha/2$ obtained from a scaling analysis [7].

So we have succeeded in extending a pervious one-dimensional numerical solution of a time fraction Stefan problem to two-dimensions. A solution that shows clear signals of anomalous transport behavior.

References

[1] J. Crank. *Free and moving boundary problems*, Clarendon Press, Oxford, 1984.

[2] J. Liu, M. Xu, Some exact solutions to Stefan problems with fractional differential equations, J. Math. Anal. Apps., 351 (2009), pp. 536-542.

[3] V.R. Voller, F Falcini, R Garra, Fractional Stefan problems exhibiting lumped and distributed latent-heat memory effects, Phys. Rev. E., 87 (2013), 042401.

[4] V.R. Voller, Fractional Stefan problems, Int. J. Heat Mass Trans., 74 (2014), pp.269-277.

[5] S. Roscani, J. Bollati, D. A. Tarzia, A new mathematical formulation for a phase change problem with a memory flux, Chaos Solitons and Fractals, (116) (2018), pp. 340-347.

[6] A. Kubica, K. Ryszewska. A selfâĂŘsimilar solution to timeâĂŘfractional Stefan problem, Math Meth Appl Sci. (2020).

[7] F. Falcini, R. Garra, V. R. Voller, Modeling anomalous heat diffusion: Comparing fractional derivative and non-linear diffusivity treatments, Int. J. Therm. Sci., 137 (2019), pp. 584-588.

Parameter Identification for a Time Fractional Parabolic System of Fractured Porous Media

Lubin G. Vulkov
Department of Applied Mathematics and Statistics,
University of Ruse "Angel Kanchev", 7017 Ruse,
Bulgaria, lvalkov@uni-ruse.bg

We consider the time fractional flow model in multicontinuum porous media

$$C_i\frac{\partial^{\alpha_i}p_i}{\partial t^{\alpha_i}} - \nabla.(k_i\nabla p_i) + \sum_{j\neq i}\eta_{ij}(p_i-p_j) + \eta_{if}(p_i-p_f) = g_i \ \text{ in } \ \Omega_T = \Omega\times(0,T), \qquad (1)$$

$\Omega \subset R^d$, $\eta_{ij} = \eta_{ji}$, coupled with fractured $(d-1)$ dimension equation

$$C_f\frac{\partial^{\alpha_f}p_f}{\partial t^{\alpha_f}} - \nabla.(k_f\nabla p_f) + \sum_{j\neq f}\eta_{jf}(p_j-p_f) = g_f \ \text{ in } \ \gamma_f = \gamma\times(0,T), \ \ \gamma\subset R^{d-1} \qquad (2)$$

$$\frac{\partial^{\alpha}p_i}{\partial t^{\alpha}} = \frac{1}{\Gamma(1-\alpha)}\int_0^t (t-s)^{-\alpha}\frac{\partial p_i}{\partial s}(s)ds, \ \ 0<\alpha\leq 1, \ \ \alpha=\alpha_1,\ldots,\alpha_I,\alpha_f,$$

the Caputo derivative is used. The unknown functions $p_i = p_i(x,t),\ x\in\Omega$, are pressure in porous or fractures matrix, $k_i\geq 0,\ k_f\geq 0$ the porous (or fracture) matrix and permeability and $\eta_{ij}=\eta_{ji}$ the mass transfer term that are proportional to the continuous permeabilities, see e.g. [1,2].

We solve the problem of *identification* of the coefficients $k \equiv \{k_1,\ldots,k_I\}$, $\eta \equiv \{\eta_{ij},\eta_{jf}\ i,j=1,\ldots,I\}$ and the initial conditions

$$\varphi(x)\equiv\{\varphi_1(x)=p_1(x,0),\ldots,\varphi_I(x)=p_I(x,0), \ \ \varphi_f(x)=p_f(x,0)\} \qquad (3)$$

if the *additional information* can be measured

$$p_i(x_l,t_m;a) = p^i_{lm}, \ \ l=1,\ldots,L, \ \ m=1,\ldots,M \qquad (4)$$

and $i\in\widehat{I}\subseteq\{1,\ldots,f\},\ a\equiv(k,\eta,\varphi\}\in A$ - the admissible set.
It can be rewritten in operator form $\mathcal{A}(a)=P$, where $\mathcal{A}: A\to\mathcal{P}$ is an injective operator, $a\in A,\ p\in\mathcal{P}$, $\mathcal{P}$ is a Euclidian space of data $P=\{p^i_{11},\ldots,p^i_{LM}\}$.

The inverse problem $\mathcal{A}(a) = p$ is **ill-posed**, i.e. its solution may not exist and/or its solution is non-unique and/or unstable to errors in measurements (3), see e.g. [2,3] . Here, the inverse problem is reduced to the minimization problem

$$a^* = arg \min_{a \in A} J(a), \quad J(a) =< \mathcal{A}(a) - p, \ \mathcal{A}(a) - p >, \tag{5}$$

where the functional $J(a)$ characterize the quadratic derivation of the model data from the experimental data. and we take it as follows

$$J(a) = \sum_{i \in \widehat{I}} \sum_{l=1}^{L} \sum_{m=1}^{M} (p_i(x_l, t_m; a) - p_{lm}^i)^2$$

By the following assertion we report the well-posedness of the direct (forward) problem.

Theorem 1 The direct problem (1),(2) with zero Neumann's boundary conditions is well-posed in appropriate functional spaces and the energy estimate holds

$$E(t) \le E(0) E_\beta(\rho_1 t^\beta) + \Gamma(\beta) E_{\beta,\beta}(\rho_1 t^\beta) D_{0t}^{-\beta} \rho_2(t), \quad \beta = \min(\alpha_1, \dots, \alpha_I, \alpha_f),$$

$$E(t) = \sum_{i=1}^{I} \int_\Omega C_i p_i^2(x,t) dx + \int_\Omega C_f p_f^2(x,t) dx, \tag{6}$$

$$\rho_2(t) = \sum_{i=1}^{I} D_{0t}^{-\alpha_i} \int_\Omega g_i^2(x,t) dx + D_{0t}^{-\alpha_f} \int_\Omega g_f^2(x,t) dx, \tag{7}$$

ρ_1 is a constant and $E_\beta, E_{\beta,\beta}$ are Mittag-Leffler functions.
The derivation uses Gronwall and Bellman type inequality and the simple one if $\beta \le \alpha$ and $h(t) \ge 0$ then

$$D_{0t}^{-\alpha} h(t) \le \frac{\Gamma(\beta) t^{\alpha - \beta}}{\Gamma(\alpha)} D_{0t}^{-\beta} h(t)$$

for the Riemann - Liouville integral.

Further, for clarity, we will consider the continuum model in [1] for $d = 1$, $I = 2$ and k_1, k_2-constants, $k_f = 0$ as well as $\eta_{12} = \eta_{21} = l(t)$, $\eta_{1f} = \eta_{f1} = b(t)$, $\eta_{2f} = \eta_{f2} = c(t)$, , i.e. we have $M = 3$ unknown reaction coefficients. Also, we will take $C_1 = C_2 = C_f = 1$, $g_1 = g_2 = g_f = 1$. Now, we can introduce the matrices with the vector $\eta = (l, b, c)$:

$$B = (b_{in}) = \begin{pmatrix} -l-b & l & b \\ l & -l-c & c \\ b & c & -b-c \end{pmatrix}, \ Q = (q_{in}) = \begin{pmatrix} -p_1+p_2 & -p_1+p_f & 0 \\ -p_2+p_1 & 0 & -p_2+p_f \\ 0 & -p_f+p_1 & -p_f+p_2 \end{pmatrix}$$

Next, if δa is an increment we denote the deviation of solution $\mathbf{p}(p_1, p_2, p_f)$ by $\delta \mathbf{p}(x, t; \delta a) = \mathbf{p}(x, t; a + \delta a) - \mathbf{p}(x, t; \delta a)$.

Then it satisfies the following initial boundary value problem with accuracy up to terms of order $o(|\delta a|^2)$, the *sensitivity* problem:

$$\frac{\partial^{\alpha_1}\delta p_1}{\partial t^{\alpha_1}} - k_1\frac{\partial^2\delta p_1}{\partial x^2} - \sum_{n=1}^{N} b_{1n}\delta p_n - \sum_{s=1}^{S} q_{1s}\delta\eta_s - \delta k_1\frac{\partial^2 p_1}{\partial x^2} = 0,$$
$$\frac{\partial^{\alpha_2}\delta p_2}{\partial t^{\alpha_2}} - k_2\frac{\partial^2\delta p_2}{\partial x^2} - \sum_{n=1}^{N} b_{2n}\delta p_n - \sum_{s=1}^{S} q_{2s}\delta\eta_s - \delta k_2\frac{\partial^2 p_2}{\partial x^2} = 0,$$
$$\frac{\partial^{\alpha_f}p_f}{\partial t^{\alpha_f}} - \sum_{n=1}^{N} b_{3n}\delta p_n - \sum_{s=1}^{S} q_{3s}\delta\eta_s - \delta k_f\frac{\partial^2 p_f}{\partial x^2} = 0,$$
$$N = I + 1 = 2 + 1 = 3, \quad S = 3, \quad p_3 = p_f.$$

$$\delta p_i(x,0) = \delta\varphi_i(x), \quad x \in \Omega = (0,1),$$
$$\left.\frac{\partial p_i}{\partial x}\right|_{x=0} = \left.\frac{\partial p_i}{\partial x}\right|_{x=1} = 0, \quad i = 1,2, \quad p_3 = p_f, \quad t \in (0,T).$$

Now we are in position to formulate our main result.

Theorem 2. The gradient of the cost functional $J(a)$ is given by

$$J'(a) = \left(\int_\Omega Q^{T_r}R(x,t)dx, \quad \int_\Omega\int_0^T \frac{\partial^2}{\partial x^2}(x,t)R(x,t)dtdx, \quad R(x,0)\right)^{T_r},$$

where the vector function $R(x,t)$ is the solution of the *adjoint problem*

$$\frac{\partial^{\alpha_1}r_1}{\partial t^{\alpha_1}} + k_1\frac{\partial^2 r_1}{\partial x^2} - \sum_{n=1}^{N} b_{n1}r_n + S_1 = 0, \quad \frac{\partial^{\alpha_2}r_2}{\partial t^{\alpha_2}} + k_2\frac{\partial^2 r_2}{\partial x^2} - \sum_{n=1}^{N} b_{n2}r_n + S_2 = 0,$$
$$\frac{\partial^{\alpha_f}r_f}{\partial t^{\alpha_f}} - \sum_{n=1}^{N} b_{n3}r_n + S_3 = 0, \quad N = I + 1 = 2 + 1 = 3, \quad p_3 = p_f,$$
$$r_i(x,T) = 0, \quad x \in \Omega; \quad \left.\frac{\partial r_i}{\partial x}\right|_{x=0} = \left.\frac{\partial r_i}{\partial x}\right|_{x=1} = 0,$$
$$S_i = \sum_{m=1}^{M}\sum_{l=1}^{L}\int_0^T\int_\Omega (p_i(x,t;a) - p_{lm}^i)\delta(t-t_m)(x-x_l)dxdt, \quad i = 1,2,3, \quad p_3 = p_f$$

and $\delta(t-t_m)$ is the Dirac-delta function.

The report focuses on the theoretical analysis of the problem. On further we will continue with the numerical solution using the CGM (Conjugate Gradient Method).

Acknowledgements This research is supported by the Bulgarian National Science Fund under the Bilateral Project KP/Russia 06/12 "Numerical methods and algorithms in the theory and applications of classical hydrodynamics and multiphase fluids in porous media" from 2020.

References

[1] A. Tyrylgin, M. Vasilyeva, A. Alikhanov, D. Sheen, A computational macroscale for the time fractional poroelasticity problem in fractured and heterogeneous media, Arhive 201.07638v1 [math.NA] 2022

[2] G. Chavent, Nonlinear Least Squares for Inverse Problems : Theoretical Foudations and Step-by-Step Guide for Applications, Springer, 2009.

[3] T.B. Gyulov, L.G. Vulkov, Reconstruction of the lumped water-to-air mass transfer coefficient from final time or time-averaged concentration measurement in a model porous media, BG SIAM,2021.